ESRF NEWSLETTER

OCTOBER 2000 EUROPEAN SYNCHROTRON RADIATION FACILITY N° 34

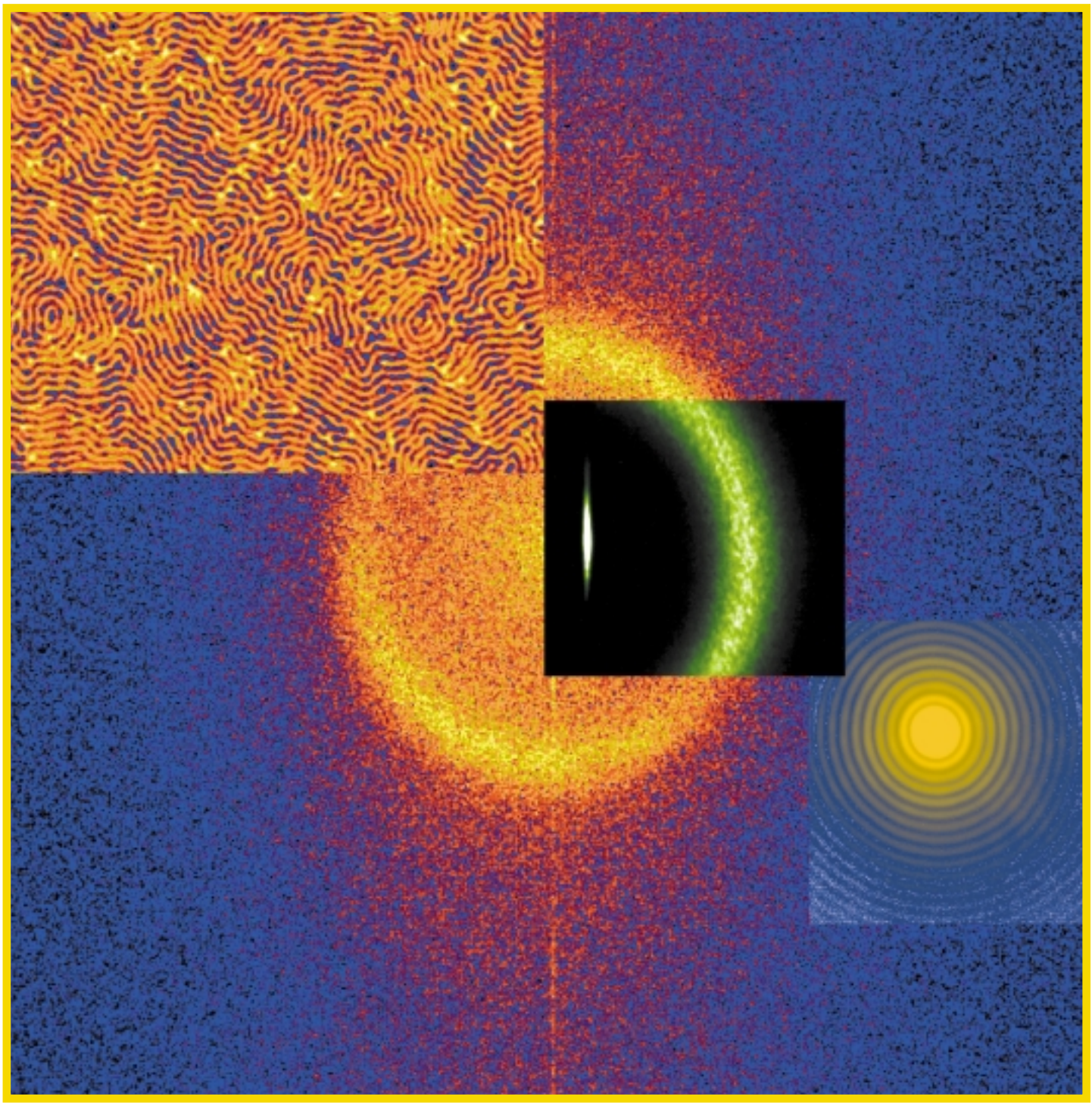

A Magnetic Force Microscopy image of the magnetic domains in $GdFe_2$ thin films (top left); the diffraction image from these domains as taken on beamline ID12B (centre); and a Fraunhofer image illustrating the nearly perfect coherence that can be obtained with soft X-rays (bottom right). In the background is the 2-D powerspectral density of the MFM picture.

ISSN 1011-9310

CONTENTS

Photography by:
C. Argoud, S. Claisse and C. Jarnias.

Professor Stirling (left) explaining the research carried out on BM28 - the British XMAS CRG beamline - to Sir M. Jay, British Ambassador to France during his visit to the ESRF in November 1998.

New Director General from 1st January 2001

The ESRF Council has appointed Professor William G. Stirling as Director General of the ESRF to succeed Yves Petroff from 1st January 2001, for a period of five years.

Professor Stirling is Professor of Experimental Physics (Condensed Matter Physics) at the University of Liverpool. His current research interests include X-ray investigations of the magnetic structures and phase transitions of magnetic materials (bulk, thin films and multilayers), which are among the core activities of the ESRF. Professor Stirling has worked on these synchrotron experiments at ESRF, NSLS, HASYLAB and Daresbury. In collaboration with Professor M.J. Cooper of the University of Warwick, Professor Stirling directs the UK CRG beamline, XMAS.

Bill Stirling is well acquainted with the Grenoble research environment since he worked at the ILL from 1973 to 1987 and was a member and chairman of the ILL Scientific Council from 1992 until 1997 and subsequently has served on the ILL Steering Committee.

HUNGARY JOINS THE ESRF

10 February 2000

On Thursday 10 February 2000, an arrangement was signed in Grenoble between the Department of Scientific Affairs of the Hungarian Ministry of Education and the ESRF concerning the scientific use of synchrotron radiation at the ESRF by Hungarian scientists. The signature took place at the occasion of the 10th ESRF Users' Meeting. The arrangement was signed by Professor Gábor Náray-Szabó (Head of the Department of Scientific Affairs of the Hungarian Ministry of Education) and by Professor Yves Petroff (Director General of the ESRF). Also present during the signing ceremony was Professor Denes Lajos Nagy, Chairman of the Hungarian Synchrotron Radiation Committee. The arrangement came into effect on 1 July 2000 and has been concluded for a duration of two years. It is expected that during this period it will be replaced by an arrangement on the long-term use of synchrotron radiation with a consortium CENTRALSYNC, assembling scientific organisations from the Czech Republic, Hungary and Poland.

K. Witte

Professor Gábor Náray-Szabó (left) and Professor Yves Petroff (right)

ESRF HOSTS ITS 10TH USERS' MEETING

10 February 2000

The ESRF hosted a very successful series of meetings around the 10th Users' Meeting last February. On 8 and 9 February, a workshop on Fast Structural Changes was coordinated by Heinz Graafsma. The aim of the workshop was to investigate the possible scientific progress that could be made if current detection limitations were overcome. The Plenary day (Thursday 10 February) was followed by two workshops, one on Self Organisation at Surfaces and Interfaces, coordinated by Detlef Smilgies, and the other on Challenging Problems in Structural Biology coordinated by Soichi Wakatsuki and Gordon Leonard. Each of them attracted approximately 100 participants, and this helped to ensure that the total number of participants over the five days exceeded 400. Since this was the tenth Users' meeting - although "Users" meetings actually started before any beam appeared - the Users' Organisation decided to offer a prize of 10 000 FF, twice the usual amount, to the winner of the Young Scientist Award. Richard Neutze, who currently works at the University of Uppsala, won the prize this year. He presented results covering picosecond biology, picosecond chemistry, and simulations of the potential for femtosecond X-ray imaging. The Plenary session talks also included four other highlights from ESRF-based research. Eric Dooryhee described the fascinating detective work done on tiny amounts of cosmetic eye-shadow taken from ancient Egyptian artefacts; Anders Liljas surveyed the crystallographic studies of ribosomes and ribosomal subunits; Rainer Luebbers discussed inelastic nuclear scattering studies of α and ε iron at pressures up to 42 GPa, and Carlo Meneghini described XAFS work on doped perovskites displaying colossal magnetoresistance. Over seventy posters were presented in a lively afternoon session. This was followed by a preview of the CD-ROM on synchrotrons and synchrotron radiation by Dominique Cornuejols. Recent results from the Medical Beamline were featured in a short talk by Bill Thomlinson, who shared a brief session in which industrial users from Unilever, L'Oréal and Aventis discussed the value of synchrotron radiation studies to their Research and Development. Our thanks to all those who helped make these days such a success.

The next Users' Meeting will be held on Monday 19 February 2001.

M. Cooper

Dr Richard Neutze, who received the 10th Users' meeting Young Scientist Award.

Beam Instability Workshop

13/15 March 2000

60 participants from 19 laboratories from around the world attended the workshop from Monday through to Wednesday, 13 to 15 March. The subject of beam instabilities concerns most machines and there have been huge developments in understanding the controlling techniques for these instabilities over the past ten years. The workshop was therefore an excellent opportunity to get up-to-date on these critical issues and to raise a number of questions of interest to the ESRF, for example, understanding instability mechanisms, use of feedback, minimisation of impedance… The workshop was organised into plenary sessions in the morning and working group discussions in the afternoon. The two working groups dealt with "high intensity per bunch" and "multibunch". The workshop was a frank success and several proposals were forthcoming: the establishment of mailing lists, crossed participation from several facilities for measurements of common interest, benchmarking the impedance of a few typical components with modelling software, installation of a test impedance in a machine, standardisation of key hardware elements etc.

D. Goodhew

Proceedings of the workshop are available on-line:
http://www.esrf.fr/machine/myweb/machine/Workshop/BIW/BIWhome.htm.

Review of the Latest Proposals for Beam Time

785 new applications for beam time arrived at the User Office for the March 1st deadline. Proposals came from labs in Europe, the USA and Japan, and from as far afield as Brazil, Korea and South Africa. A total of 12 529 shifts of beam time were requested for the current scheduling period, from August 2000 to mid February 2001.

The distribution of proposals across major scientific areas for this review round is shown in the figure below. The nine Review Committees which met on 27 and 28 April 2000 selected 364 proposals (46.4%) which were allocated beam time totalling 5 904 shifts.

R. Mason

Surfaces and Interfaces	**8 %**
Chemistry	**14 %**
Hard Condensed Matter: **Elect. & Magn. Properties**	**16 %**
Hard Condensed Matter: **Structures**	**19 %**
Materials Eng. & Environmental Matters	**11 %**
Life Sciences	**16 %**
Methods and Instrumentation	**7 %**
Soft Condensed Matter	**9 %**

ESRF Workshop for Industry: Powder diffraction on Pharmaceuticals

29 March 2000

The ESRF was pleased to welcome a dozen participants for the workshop dedicated to the characterisation of pharmaceuticals by powder diffraction. The aim of this meeting was to give the participants an opportunity to discover the facilities of the ESRF and its potential in this important and highly specialised domain. Participants came from major European companies, such as Servier, Novartis, Glaxo Wellcome, Boehringer, Pierre Fabre and Laboratoire Fournier, as well as from smaller companies or university laboratories working in this field.

The programme began with scientific presentations: P.F. Lindley, Research Director, presented an outline of the ESRF, in which he explained the production of synchrotron light and the interest of the third generation sources. He also showed the reliability of the beam, an important parameter for industrialists, and described the different beamlines and their status. Then, A. Kvick, Head of the Diffraction Group, and A. Fitch, scientist in charge of BM16, gave two presentations dedicated to the description of ID11 and BM16 beamlines and their use in the study of pharmaceutical powders. They explained that the brightness and high resolution of the ESRF beams allow more information to be extracted from powder diffraction than when using a classic X-ray laboratory source. The ESRF powder diffraction setups permit the measurement of the utmost high-resolution data for solving crystal structures, for quantitative phase analysis or real-time studies. Such precision is of prime importance in the study of polymorphism, stability during storage and structural changes that are induced either by temperature, hydration and other physico-chemical parameters, or after industrial processes like milling, drying, grinding and tableting. Important also is the ability to make a highly accurate comparison of the crystalline forms of a generic drug with that of its original form. Finally, of great interest to the participants was the possibility of determining the crystalline structure from small crystals with dimensions as small as 10 μm instead of powders, which considerably increases the chance of success.

After a guided tour of the facilities, the Industrial Co-ordinator gave a brief final presentation. He described the various access modes to the ESRF that are offered to the industrialists and gave an outline of a future service for powder diffraction on pharmaceuticals.

Following this workshop, the ESRF has received requests for analysis from half a dozen companies.

J. Doucet

Open Days

20-21 May 2000

The ESRF, ILL and EMBL opened their doors to the public on the 20 and 21 May. Almost 1400 visitors came to discover the three research facilities. They were not disappointed as the staff who participated in these open days did their best to make it a very enjoyable and interesting occasion for all. In fact some of visitors who came on Saturday were so enthusiastic that they asked whether it was possible to come back on Sunday as well. The programme proposed at the ESRF permitted visitors to discover the various animated areas at their own pace, and, for some, half a day did not seem to be enough for a complete visit. After discovering the storage ring from the roof of the tunnel, our visitors were invited to learn about the secret of the resistance of spider silk on ID13, to admire the protein structures studied on ID14 and to listen to the explanations given by the staff of the Medical Beamline (ID17).

Visitors gathering around the scale model of the ESRF.

C. Argoud

Workshop on the Structure and Dynamics of the Liquid and Glassy States

22/23 May 2000

On Monday 22 and Tuesday 23 May, the ESRF played host to a workshop on "The Structure and Dynamics of the Liquid and Glassy States: X-ray and complementary methods". Approximately 80 participants united by a common interest in the science of structurally disordered condensed matter systems, enjoyed a workshop programme of 20 oral presentations and a lively poster session with over 30 high quality contributions. Throughout this event, emphasis was placed on active audience participation and the programme was thus constructed to give ample room for lively scientific discussion and debate. It was pleasing to note that through the additional sponsorship provided by the Liquid Matter Network of the UK Engineering and Physical Sciences Research Council and the Gruppo Nazionale di Struttura della Materia of the Italian Consiglio Natzionale delle Ricerche, a considerable number of young scientists, students and postdocs were able to attend this event. In fact, young scientists accounted for approximately 25% of the total workshop participants.

The scientific conclusions drawn from this workshop were wide ranging and highlighted several of the possibilities now raised by the powerful instrument suites of third generation synchrotron sources. However, perhaps the most important message that the participants were urged to take away with them, was that progress in this complex field of research can only be made through a holistic experimental approach - in particular (and by no means exclusively) through the combination of neutron, X-ray and computational methods.

D.T. Bowron

Dr Paul-Erich Zinsli, New Chairman of the ESRF Council.

Paul-Erich Zinsli, New Chairman of the ESRF Council

Since January 1, 2000, the ESRF Council has been chaired by Dr. Paul-Erich Zinsli, from Switzerland, who was elected by Council for a period of two years at its 31st meeting on June 7 and 8, 1999. He succeeds Georg von Klitzing, Chairman in 1998 and 1999.

Paul-Erich Zinsli, 56, has been Head of the Swiss Delegation to the ESRF since 1988 and Vice-Chairman of the ESRF Council from 1998 to 1999.

He is a physicist by training and did research in gamma-ray detectors, time-resolved and low-temperature spectroscopy and molecular dynamics at UCLA and at the University of Bern. In 1980 P.-E. Zinsli joined the Federal Office for Education and Science in Bern where today he is the Deputy Director. His responsibilities cover research policy and planning as well as the financial support of national research institutions, of international organisations (CERN, ESO, ESRF, ILL, ...) and of international programmes (EU-Programmes, COST).

In international organisations, P.-E. Zinsli represents Switzerland e.g. in the Steering Committee of ILL, in the OECD Global Science Forum and in EU Fusion Research Committees.

The new Vice-Chairman of the ESRF Council is Robert Comès, Director of the Laboratoire pour l'utilisation du rayonnement électro-magnetique (LURE).

K. Witte

32ND AND 33RD MEETINGS OF THE COUNCIL

1/2 December 1999 and 5/6 June 2000

At its two most recent meetings, the Council decided several items of importance for the scientific and organisational future of the facility.

Scientific matters and arrangements with third parties

As reported earlier, the ESRF has rebuilt its Multiple Wavelength Anomalous Dispersion (MAD) beamline (BM14) at an insertion device location (ID29). The Council endorsed Management's proposal for transforming beamline BM14 into a CRG beamline with a view to keeping it in operation as a MAD beamline for protein crystallography, and recovering its construction costs for the beamline refurbishment budget. Given that two groups were interested, one from Spain and one from the UK, the Council endorsed a collaborative agreement between these two groups: for a transition period of two years, during which a further bending magnet beamline for macromolecular studies will be installed, the Spanish and the UK CRGs each obtain 50 % of the beamtime at BM14; afterwards the normal distribution of 1/3 for ESRF users and 2/3 for CRG users will be re-established at each of the two new CRG beamlines.

The Council noted the planned transfer of the powder diffraction facility from BM16 to an insertion device which will permit an increase in performance and, at the same time, provide the second bending magnet beamline for the above mentioned CRG groups mentioned above.

The Council agreed that medium-term arrangements on the use of the ESRF may be concluded with institutes from Poland and Hungary for a period of two years, along the lines of the arrangement concluded with the Institute of Physics of the Czech Academy of Sciences (the arrangement with Hungary was signed on 10th February 2000 and came into effect on 1st July 2000). It approved the extension for a further five years of the contracts with the Collaborating Research Groups SNBL, D2AM, GILDA and IF, concerning the operation of the beamlines BM1, BM2, BM8 and BM32 respectively.

With a view to a better continuity in the staffing of the beamline teams, the Council raised the maximum number of permanent scientific appointments from 30 to 35. In addition, the Council agreed that some flexibility be introduced between the numbers of posts for fixed-term scientific appointments (beamline scientists, post-docs, thesis students, altogether about 120).

Legal, procedural and financial matters

The Council noted the scientific use made of the ESRF over the six recent allocation periods, concluded that there was a significant and lasting imbalance between scientific use and contributions, and decided with a qualified majority (the Nordsync delegation voting against) that corrective measures were appropriate. To prepare such corrective actions a working group has been established (which had its first meeting on 14 September 2000).

Based on its industrial policy statement of June 1999, the Council adopted new guidelines for the use of the ESRF by industrial companies and new guidelines for licence agreements.

The new French legislation concerning the reduction of the working time had led to in-depth discussions between Management and staff on the work organisation. The Council endorsed by majority the agreement on the implementation of the 35-hour week legislation that the Director General had signed with two Unions, and confirmed at this occasion that, in accordance with §12.1 of the ESRF Statutes, a close link should be maintained between the salaries of the ESRF staff and those of the French Commissariat à l'Energie Atomique.

The Council took note of the final accounting of the construction period (1988-1998) and of the final adjustments of contributions between France, Germany, Italy and UK resulting therefrom. It approved, with the Italian delegation abstaining, the budget for 2000, providing for an expenditure of 436 245 kFF (66 505.12 kEuro) in payments and requiring Members' contributions of 404 000 kFF (61 589.40 kEuro).

The Council asked Management to remove the contribution of the Scientific Associate Portugal towards previous construction costs from the income figures in the budget and the medium-term financial estimates but appealed to Delegations to maintain their shares in these Portuguese back payments on their accounts for a possible later user with a view to an expansion of the experimental programme. It took note of the correspondingly revised medium-term financial estimates for the period from 2001 to 2005 and agreed the principles for the utilisation of additional income (e.g. from the sale of BM14 and BM16) embodied therein (i.e. re-investment into the beamline programme).

Appointment of Directors and Chairpersons

The Council

- elected Robert Comès as its Vice-Chairman for the period from 1st January 2000 to 31st December 2001;
- appointed William G. Stirling as Director General for the period from 1st January 2001 to 31st December 2005;
- approved that the appointment of Director of Research from 1st October 2001 (in succession to Christof Kunz) to 30th September 2006 be offered to Francesco Sette;
- approved job descriptions and adopted procedures for seeking candidates for appointment as Machine Director from January 2002, as Director of Administration from February 2002 and as Director of Research (succession of Peter Lindley) from June 2002.

K. Witte

HERCULES

Celebrates Its 10th Anniversary

The H.E.R.C.U.L.E.S. (Higher European Research Course for Users of Large Experimental Systems) course has been running now for ten years. Since the beginning of the project in 1991, more than 1200 applications were received, from which over 700 participants were selected. The participants were either Ph.D students or post-doctoral scientists who use large-scale neutron or synchrotron radiation facilities in their research. The high number of applicants demonstrates that this training programme answers a need expressed Europe-wide. The participants actually came from 18 European countries (**Figure 1**). The opportunity to participate in the course has been given to non-European candidates since 1998 for the Biological session and from this year for the Physics and Chemistry session. This enabled the particpation of students from China, the United States, Brazil and Argentina.

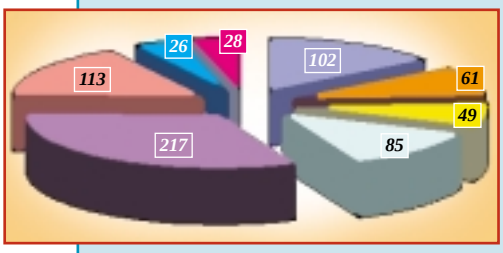

Germany
Spain
Great Britain
Italy
France
Other EU countries
Eastern countries
Others

Fig. 1: Number of participants per country.

The success of the six-week course comes from the careful balance between lectures from internationally renowned experts, practical work at the large-scale facilities (about 40% of the programme), tutorials with local scientists, a poster session and visits to the installations. Since 1991 each session has welcomed an average of 70 participants, of whom over 80% followed the training full-time, while the remainder attended only the lectures and classwork (**Figure 2**). In 2000, there were 65 full-time participants, 44 in Physics-Chemistry and 21 in Biology, and there were also 12 part-time participants.

Each year the lectures were given by about 60 European speakers, who are leading specialists in their respective fields. An additional 100 research scientists and teachers took charge of the practical sessions and classwork. Most of the teachers came from the local scientific community and represented a wide range of nationalities, since several of the large-scale facilities or host laboratories, such as the ESRF, ILL and EMBL, are multinational (**Figure 3**). In groups of 4, the participants received 50 hours of personalised training. It was an excellent opportunity for participants to establish contact with the scientists at the large-scale facilities, and hence to become familiar with the potential existing there.

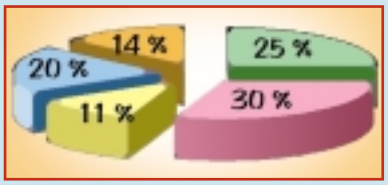

ILL-ESRF
France
Germany
Great Britain
Others

Fig. 3: Origin of the lecturers.

On the tenth anniversary of the HERCULES course, the associated HERCULES X Euroconference took place at the ATRIA World Trade Center in Grenoble and at the ESRF/ILL site, between 6 and 9 April 2000. Special thanks go to I. Anderson (ILL) and V. Guerard (CNRS) for their precious help in the organisation of this event. More than 200 HERCULES students, both past and present, participated in the conference. By bringing together these young scientists with carefully selected key-note lecturers and local researchers from the large European facilities (ESRF and ILL), the conference provided a unique training environment emphasising the latest developments and applications in the various fields, some of which are not yet covered by the course.

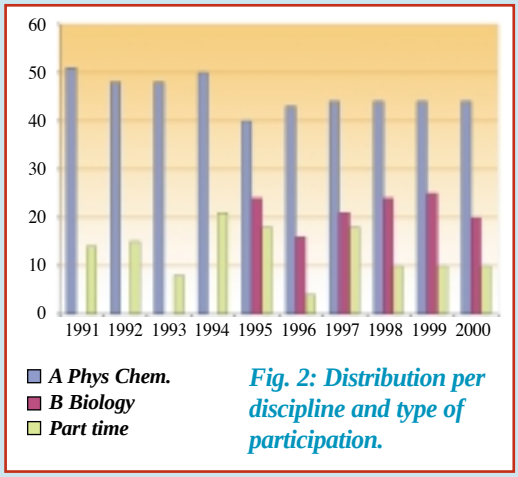

A Phys Chem.
B Biology
Part time

Fig. 2: Distribution per discipline and type of participation.

Euroconference Programme

The programme of the conference was structured to highlight the impact of fundamental and technological breakthroughs in research centred at large scale facilities using synchrotron radiation and neutrons. Internationally reputed scientists gave plenary lectures presenting the state of the art and recent developments. There were five major themes: Macromolecular biology, Magnetism, Imaging and Coherence, New Techniques, New Instrumentation and Industrial Applications. All of the oral sessions were well balanced with contributions from both senior scientists and former HERCULES students. This was a very good way of gathering together confirmed and new experts. The plenary lectures were complemented by poster contributions covering a wide range of research topics including: Materials Science, Environmental Science, Surfaces and

HERCULES X Euroconference attendees take advantage of the poster sessions to renew or create contacts and collaborations.

Interfaces, Soft Condensed Matter, Disordered systems. Each poster session was introduced by parallel "clip sessions" in which participants briefly presented their contribution.

The conference started with a short welcoming address by C. Feuerstein, President of Grenoble Scientific University, in the presence of several personalities such as H. Curien, past French Minister of Research, an EU representative, the Mayor of Grenoble, and representatives from various sponsoring scientific institutions. Then a short history of HERCULES was presented from both the inside, by J.R. Regnard, Director of the course and Chairman of the HERCULES X EuroConference, and the outside, by Y. Petroff, Director General of the ESRF.

Chaired successively by P. Day, H. Curien and D. Raoux, the scientific session of the first day opened with the latest developments on medical synchrotron research by W. Thomlinson (NSLS and ESRF) who also presented the first real experiments performed at the ESRF in collaboration with the Grenoble Hospital. Then applications of synchrotron radiation in magnetism and imaging with coherent X-ray beams were introduced successively by M. Altarelli (Director of ELETTRA-Trieste) and P. Cloetens (former HERCULES scientist and former ESRF Young Scientist Prize Winner). F. Mezei (HMI-Berlin) also explained why we need neutrons in the 21st Century, and M. Mezouar, a HERCULES scientist, presented the latest results obtained at the ESRF under extreme conditions. On this and the following day, a large poster session made it possible for all former HERCULES participants to present their work. This first day ended with a session dedicated to new instrumentation and techniques which was presented by two former HERCULES participants: P. Høghøj and M. Krisch, who spoke about multilayers for neutrons and inelastic X-ray scattering, respectively.

The morning of the second day was dedicated to industrial applications. An overview of applied and industrial research at neutron and SR facilities was given by J. Doucet (ESRF and LURE), followed by examples of investigations on biological molecules of industrial interest, presented by F. Winkler (Hoffman La Roche and Paul Scherrer Institut). J. Webster (Mat. Eng., Univ of Salford) and J. Pannetier (Corning SA) described applications of neutrons and synchrotron radiation to residual stress measurements and to industrial problems in chemistry. This industrial session, chaired by Y. Petroff, ended with a presentation by F. Comin (ESRF)

Some official attendees at the HERCULES X Euroconference: (from left to right, first row) H. Curien, past French Minister of Research, C. Feuerstein, President of Grenoble's Scientific University, Y. Petroff, Director General of the ESRF, J.R. Regnard, Chairman of the Euroconference, (second row) R. Maynard, Ministry of Education, C. Kunz, Scientific Director of the ESRF, J.X. Boucherle, Grenoble City Council, J. Baruchel, co-Chairman of the Euroconference.

on the first ESRF beamline dedicated to industrial semiconductor applications, and by R. Simon (HERCULES scientist) on a customer oriented SR source: ANKA.

The imaging and coherence session was introduced by two HERCULES scientists: J. Susini and T. Weitkamp, followed by G. Grübel (ESRF) and G. Schneider (Univ. Göttingen and BESSY). It covered scattering with coherent X-ray beams, X-ray microbeams, full-field imaging, tomography and X-ray microscopy. New projects, such as the X-ray free electron laser, were presented by J. Schneider (Director of the XFEL Project, DESY, Hamburg).

On the Saturday, the biology session was introduced with an overview on structural genomics by P. Umbach (Berlin). Several structural biocrystallography contributions were given by HERCULES scientists: A. Royant, J. Perez, C. Branca, as well as a presentation on a molecular rotary motor: ATP synthase, given by A. Leslie (Cambridge). Finally an account of muscle and fibre diffraction was animated by K. Holmes (Heidelberg). The magnetism session opened with a comparison of neutron and synchrotron X-ray results by C. Vettier (co-Director of ILL), followed by neutron results on bulk or magnetic thin films and multilayers presented by H. Zabel (Univ. Bochum) and M.R. Eskildsen (HERCULES Scientist). Example of XMCD analysis was also given by a HERCULES scientist, S. Andrieu.

The final session, focused on the latest instrumentation developments, was presented mainly by HERCULES scientists: T. Ursby, E. Lelièvre-Berna, H. Birkedal and S. Pascarelli, who closed the scientific contributions with a talk entitled "what I have learnt about EXAFS since HERCULES 1st".

The conclusions of the conference, presented by J. Baruchel (ESRF), showed that this international, multidisciplinary assembly of recently trained young researchers and leading scientists from the community generated a cross talk of new ideas on fields of applications, and helped to define the future training requirements on a European level. Furthermore this conference provided a unique occasion for former HERCULES students to mix together, renew or create contacts and collaborations at an international level. This event also gave the opportunity of launching a WEB based network of HERCULES students, to which a large number of the participants have registered. This network will provide an important means of perpetuating the European links created by HERCULES.

The Wine & Cheese party.

The proceedings of the scientific presentations have been published. The HERCULES X EuroConference was also the opportunity to print a leaflet: '10 years of HERCULES' which gives a condensed report on the activity of the Course from 1991 to 2000. These documents can be obtained on request from the HERCULES organisers.

As for the usual HERCULES courses, the schedule was tight; however, there was time for participants to exchange scientific and non-scientific ideas, and to join in common musical and dancing experiments with the help of a dynamic jazz orchestra "Cameleon". This unscheduled training session took place during the banquet organised on the first day at the "Château de Sassenage" where the participants were treated to a delightful taste of European culture and culinary expertise: it was a huge success. Finally, to give a delicate French touch to this conference, the concluding session ended with a wine and cheese party offering a large palette of different wines and more than 50 different French cheeses!

Following this highly satisfactory conclusion of this 10 year "Herculean" task, the HERCULES courses will, of course, continue. Please see the announcement below for further details.

J-L. Hodeau

HERCULES 2001

HIGHER EUROPEAN RESEARCH COURSE FOR USERS OF LARGE EXPERIMENTAL SYSTEMS

Grenoble, 4 March - 11 April 2001

Session A:
"Neutron and synchrotron radiation for physics and chemistry of condensed matter"

Session B:
"Neutron and synchrotron radiation for biomolecular structure and dynamics"

Information:
Secrétariat HERCULES
CNRS - Maison des Magistères
BP 166 - 38042 Grenoble Cedex 9
Tel: 33 (0)4 76 88 79 86
Fax: 33 (0)4 76 88 79 81
e-mail: marie-claude.moissenet@polycnrs-gre.fr
http://www.polycnrs-gre.fr/hercules.html

Deadline for application: 20 October 2000

HARD X-RAY HOLOGRAPHY AT THE ESRF

M. BELAKHOVSKY[1], G. FAIGEL[2], S. MARCHESINI[1], M. TEGZE[2] AND O. ULRICH[1]

1 SP2M / CEA-GRENOBLE (FRANCE)

2 RESEARCH INSTITUTE FOR SOLID STATE PHYSICS AND OPTICS, BUDAPEST (HUNGARY)

Hard X-ray holography permits the visualisation of the 3-D arrangement of atoms at the angstrom level. The development and future prospects of this new technique are described.

INTRODUCTION

The knowledge of atomic and molecular structures is fundamental to physics, chemistry and biology. From the beginning of this century, much effort has been put into the development of reliable methods for structure determination. Diffraction techniques are the most common and the most highly developed for structural studies. However, not all of the problems can be solved by diffraction: well-known difficulties are that single crystals cannot be grown for all substances, and that a full structure determination is difficult from powder data alone. Sometimes the phase problem causes diffraction to fail – even with single crystals. As for non-periodic systems, like amorphous materials, quasi crystals etc., detailed structural information cannot be derived easily. Further difficulties arise with new artificial materials, which have structures that cannot always be solved by traditional crystallographic methods. Examples are the study of the local environment of low-concentration impurities in a sample, the atomic order in buried interfaces, and the atomic environment of surface adsorbates.

Therefore, it is not surprising that scientists are trying to find new techniques for structural investigations. Recently, atomic-resolution X-ray holography has emerged. It is based on the same principles as traditional holography with light: i.e. a coherent wave (called the reference wave) illuminates the object and the detector surface. The intensity modulation caused by the interference between the reference wave and the wave scattered by the object (called the object wave) is recorded. This interference pattern contains both the phase and the magnitude information of the object wave. Therefore, the original wavefront can be reconstructed, giving the 3-D spatial arrangement of the objects. Although holography is used in many areas of science and everyday life, atoms in solids could not be imaged until recently. This is because the resolution is limited by the pixel size of the detector and the size of source, in addition to the wavelength. While it is relatively easy to decrease the wavelength to the Angstrom level, giving the possibility of atomic resolution, it is difficult to reduce the source size or to increase the detector's resolution. Abraham Szöke pointed out that individual atoms in a solid could be used as sources of radiation [1]. Based on his idea, experiments were performed, first using electrons [2] and later using photons [3] as hologram forming waves. Moreover, Gog and co-workers showed that the atoms present in a sample could be used as detectors instead of sources of radiation [4]. In spite of these pioneering efforts, many problems relating to the experiment and evaluation of results remained to be solved. The most significant ones were the long measuring time, the experimental setup for synchrotron studies, background correction, and the method of reconstruction.

These problems prompted us to start a series of experiments at the ESRF. Our aim was to develop a prototype experimental setup for synchrotron holographic studies and at the same time to find reliable methods for background correction and reconstruction. In this article we would like to describe the most important results from these experiments. For clarity, first the principle of the "inside source and detector" holography is given. In our experiments the electronic system of the atoms is used as sources or detectors of X-ray radiation. Figure 1a shows the formation of a hologram in the case where the atoms act as point sources. A central atom is excited by an external

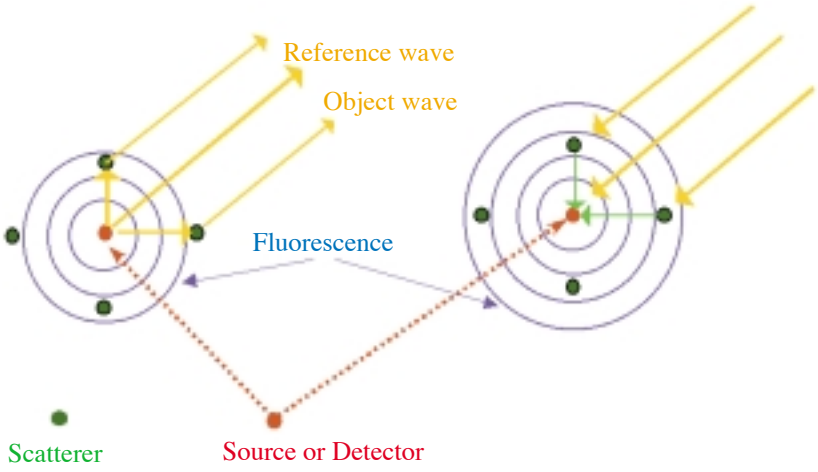

a) Direct method **b) Inverse method**

Fig. 1: The XFH principle for (a) inside "source" and (b) "detector" holography.

source. In the de-excitation process, a fluorescent photon is emitted in the form of a spherical wave. This wave can reach the detector surface directly or after scattering by the neighbouring atoms. The two waves interfere producing an intensity modulation which is measured on a spherical surface surrounding the sample. The intensity modulation contains the hologram. In the other case i.e. when atoms are used as "point detectors" the external wave is incident to the sample in the form of a plane wave (Figure 1b). This can reach the central atom directly or by scattering on the neighbouring atoms. The two waves interfere at the detector atom (central atom) and the resulting field excites the electronic system. The probability of excitation is proportional to the strength of the field. Changing the direction of the incident radiation changes the phase relation between the direct and scattered waves resulting in oscillations of the fluorescent intensity. These oscillations contain the holographic information [5].

EXPERIMENTAL DEVELOPMENTS

It is clear from the above description, that the two types of measurements require a similar experimental setup. The main difference is that in the inside source case the fluorescent radiation has to be measured as a function of the detector position in relation to the sample. While using the atoms as "point detectors" the direction of the incident beam has to be varied and the external detector has to collect the fluorescent photons from the full solid angle about the sample. The first step in our work was to develop the proper experimental setup for synchrotron measurements. It was constructed in a way that both inside "source and detector" holographic experiments could be done without remounting the sample. One of the critical components of the setup is the detection system. This should satisfy three conditions: first it has to discriminate the fluorescent photons from a relatively high background, second its angular acceptance has to be variable from the 1*1 degree^2 to the full solid angle (or as large a solid angle as possible), third it has to handle high count rates without appreciable dead time. The mechanics is another crucial part of the experimental setup. Although angular positioning and reproducibility do not have to be extremely precise, it does have to be fast - capable of 10 turns/second for one of the axes. For the two other axes rotation speed can be slower, about 2 degrees/second, but they both have to carry relatively heavy loads (3 kg). The third part of the experimental setup which needs attention is the data acquisition system. During the fast motion one has to read several counters in quick succession (every 200 microseconds).

We developed a setup which satisfies the above conditions, improving the system after every experimental run. Here we will not describe all the steps but instead present the latest version of the setup which uses the full power of synchrotron undulator radiation. The experiments were done at beamlines **ID32**, **ID18** and **ID22**.

The experimental setup is shown in Figure 2, and a description of its characteristics follows. The optics are the least complicated part. A given harmonic of an undulator is used without monochromatisation since a small bandwidth is unnecessary. However, a mirror and an absorber are needed in order to single out a given harmonic – the so-called “pink” beam – which then passes through a thin foil, which scatters part of the incident beam. The scattered radiation is used for incident beam monitoring. The mechanical system comprises two coaxial vertical rotation stages (θ, θ') coupled in such a way that the lower goniometer (θ) carries the upper one (θ'). The upper goniometer in turn holds another smaller one with a horizontal axis (ϕ). The sample is fixed to this horizontal rotation stage so that its flat surface is perpendicular to this axis when illuminated by the X-ray beam. The detector is mounted on the lower goniometer. The third part of the experimental setup is the detector assembly. Since the count rate is very high, it could not be handled by single photon counters. Therefore, we used a Si diode in the current mode. However, this does not have energy resolution, which is necessary to suppress the unwanted radiation, so the energy

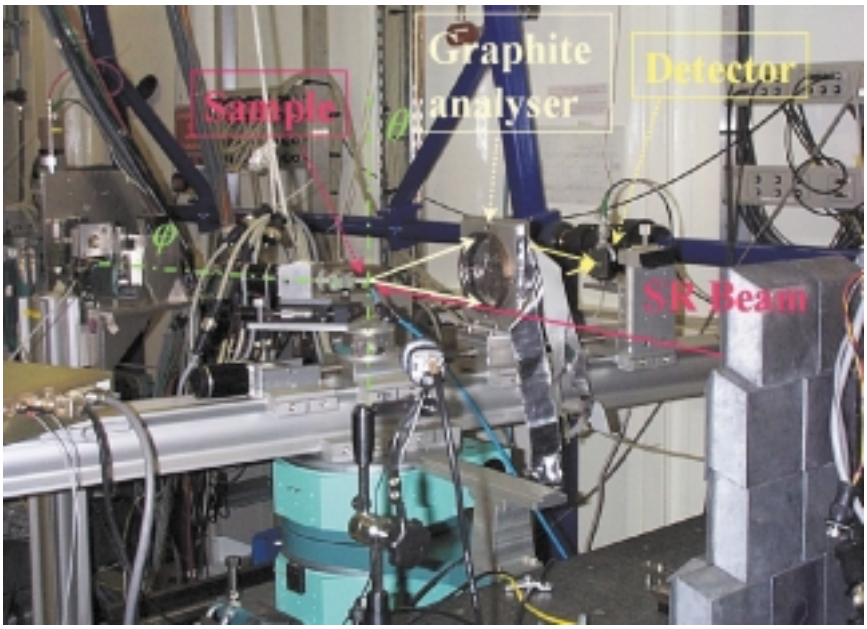

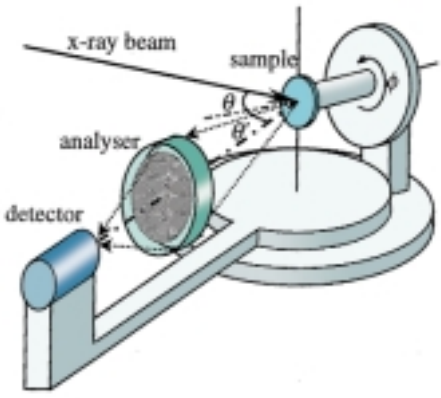

Fig. 2: Sketch of the experimental setup installed at the ESRF for the study of hard X-ray holographic measurements.

analysis was done before the detector by a doubly focusing pyrolithic graphite monochromator (Figure 2 [6]). This arrangement resulted in a large loss of detection solid angle compared to the laboratory measurements. Fortunately, this was more than compensated for by the high flux of synchrotron radiation. Typical estimated count rates were in the range of 10^{10} counts per second. Taking into account the statistical noise only, this would result in measuring times of a few seconds. However, the mechanical motion of the sample-detector system is not fast enough to scan a hemisphere in this short time. Therefore, the collection of a holographic data set at a single energy takes a few minutes.

HOLOGRAPHIC IMAGES

In the following part we would like to present a few examples of holographic imaging. Useful information can be derived from the holograms without any back-transformation. Since we use the atoms as point sources or detectors in the hologram forming process, the hologram shows the local symmetry of their environments. This is illustrated in Figure 3. The pictures show the recorded fluorescence intensities, projected on the sample surface of the upper hemisphere, after absorption correction. What is really seen is the standing wave patterns (or Kossel lines) rather than the holograms themselves, since the holographic oscillations are of much smaller amplitude. The pictures a, b and c were taken from samples having a three, four and five-fold symmetry axis perpendicular to their surface, respectively from an NiO[111] single crystal, an epitaxial FePt $L1_0$ film and an AlPdMn quasi-crystal. One can find other off-perpendicular symmetry points on these holograms from which the full local symmetry of the site can be deduced [7].

Of course, what we are finally interested in is the 3-D arrangement of atoms in real space. The next two figures show an example of this. The holograms of a CoO[111] sample are shown at four different energies (Figure 4). The reconstructed image of the Co atoms can be seen in Figure 5 [7]. In the evaluation process all four holograms were used to build a single high-resolution atomic structure. We would like to point out that

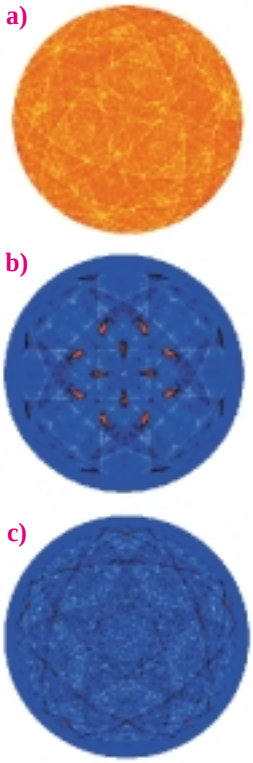

Fig. 3: Holograms and standing wave line patterns taken from samples having their surface parallel to crystallographic plane with 3 (NiO), 4 (FePt) and 5 (AlPdMn) fold axis. The FePt epitaxial film was prepared with A. Marty and B. Gilles, the quasi-crystal was supplied by F. Schmithusen and J. Chevrier.

Fig. 4: Holograms of CoO taken at energies 6925, 13861, 17444, 18915 eV respectively.

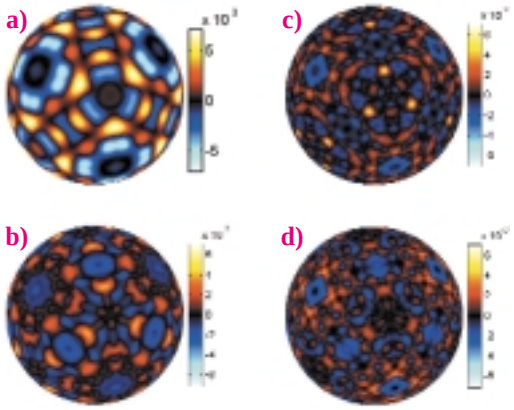

Fig. 5: The 3-D arrangement of Co atoms reconstructed from the holograms of Figure 4.

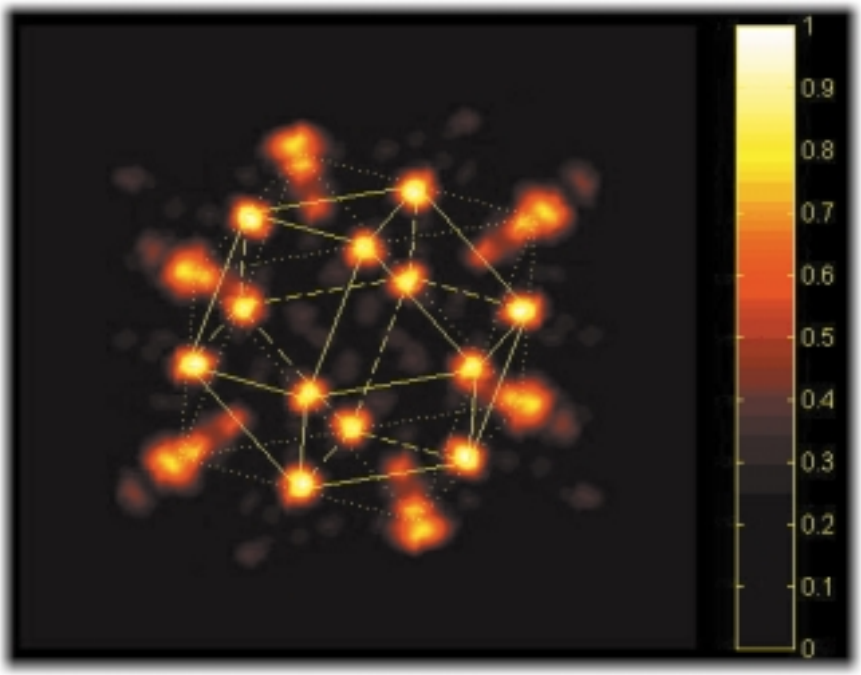

in this case the resolution is isotropic in contrast to all previous measurements, and its value (0.5 Å) is near to the diffraction limit.

FUTURE TRENDS

In spite of the substantial progress in the experimental and evaluation methods, there are many problems which need to be solved before the widespread application of this technique. Let us start with the easiest one to solve: the collection time of a hologram, which at a single energy is between 5 and 30 minutes. This does not seem too long, especially when compared with the duration of the first demonstration experiment (two months [3]). However, it would be advantageous to decrease the measuring time to 1 minute or below. The reason for this is that many artifacts inherent to holographic reconstruction can be eliminated by measuring the same sample at several (in the order of 10) energies [4,5,7]. In practical terms this would result in measuring a full data set for holographic reconstruction in 10 minutes instead of a few hours. The second problem is that we are unable to image light atoms. In all experiments so far, only relatively heavy atoms (from iron up) could be imaged. However, in many applications especially in the case of biological samples, it would be crucial to see O, C, N etc. The third problem that hinders wider application of holography is the form of the sample. Presently single crystal samples with a large (5*5 mm^2) flat surface can be measured. It would be very useful to extend the capabilities of holographic imaging to small (~10^{-3} mm^3) arbitrarily shaped crystallites.

Of course there are many other areas where holography could be improved, but we stop here after mentioning the three most important ones. We have continued to work on the above mentioned problems, and have promising results, especially on the measuring time, on the reconstructed cluster size and the imaging of light atoms [8] and on the first application to thin films. ■

REFERENCES

[1] A. Szöke, in Short Wavelength Coherent Radiation: Generation and Applications, *AIP Conference Proc., ed. D.T. Attwood and J. Boker (New York) 147, 361 (1986).*

[2] G.R. Harp, D.K. Saldin, B.P. Tonner, Phys. Rev. Lett., 65, 1012 (1990).

[3] M. Tegze, G. Faigel, Nature, 380, 49 (1996).

[4] T. Gog et al., Phys. Rev. Lett., 76, 3132 (1996).

[5] For a more detailed discussion of atomic resolution X-ray holography see: G. Faigel, M. Tegze, Rep. Prog. Phys., 62, 355-392 (1999).

[6] S. Marchesini, M. Belakhovsky, A.K. Freund, in Crystal and Multilayer Optics, SPIE proc., 3448, 224 (1998).

[7] M. Tegze, G. Faigel, S. Marchesini, M. Belakhovsky, A.I. Chumakov, Phys. Rev. Lett., 82, 4847 (1999).

[8] M. Tegze, G. Faigel, S. Marchesini, M. Belakhovsky, O. Ulrich, Nature, in print.

ACKNOWLEDGEMENTS

We would like to thank the beamline staff at ID32, ID18, and ID22 for their assistance, especially A.I. Chumakov, L. Ortega and A. Simionovici. S.M. acknowledges the E.U. Marie Curie Fellowship under grant n° ERBFMBICT961366. This work was also supported by Balaton P.A.I. n° 98024 and OTKA T022041.

APPOINTMENT OF A DIRECTOR OF ADMINISTRATION AND A DIRECTOR OF RESEARCH

The ESRF Council has opened the selection procedure for the appointment of

- **a Director of Administration** (from 1 February 2002) and
- **one of the ESRF's two Directors of Research** (from 1 June 2002).

Both appointments are for periods of five years.

For the time being, the eight delegations to the ESRF Council are invited to nominate candidates. People interested in contributing to this phase, for example by suggesting candidates, are invited to contact one of the Heads of Delegation before mid November 2000. (The Council aims at having completed the recruitment for these positions one year before the start of the appointments.)

Further information on the ESRF, on the posts and on the procedure (notably the e-mail addresses of the Heads of Delegation) can be found on the ESRF web site at **http://www.esrf.fr.**

MAGNETIC SPECKLES WITH SOFT X-RAYS

J.F. PETERS, M.A. DE VRIES, J. MIGUEL, O. TOULEMONDE AND J.B. GOEDKOOP

VAN DER WAALS-ZEEMAN INSTITUTE, UNIVERSITY OF AMSTERDAM (THE NETHERLANDS)

Soft X-rays are rare at the ESRF. Nevertheless, the ESRF's soft X-ray user community has a clear impact on synchrotron radiation research due to the capabilities of the source. In this article we want to highlight new developments in magnetic soft X-ray scattering.

Traditionally, soft X-rays are applied in biology, chemistry and physics in various forms of high-energy spectroscopies and microscopy. While these techniques are still important, there is a growing attention for soft X-ray scattering. This may seem surprising, since the wavelengths in question, 5 Å and longer, are too large to fit interatomic distances. However, they do fit the length scales involved in the blooming field of 'nanoscience', as well as the correlation lengths occurring in many solids, such as superconductors and magnetic materials. Usually this size range is addressed by small-angle scattering (SAX) at hard X-ray energies (E > 5 keV). Because of the very high absorption coefficients at longer wavelengths, soft X-ray scattering is a technical challenge, requiring complicated vacuum beamlines, vacuum diffractometers, and thin samples.

WHENCE THEN THE ATTENTION FOR SOFT X-RAY SCATTERING?

The answer is found precisely in those strong absorption effects. By tuning the X-ray energy to an absorption resonance of a *specific* element, one can obtain a large increase in the sensitivity to that element. Furthermore, magnetic or crystal field effects that break the spherical symmetry of the atom give rise to *polarisation*-dependent scattering effects. Resonant scattering experiments are possible at the absorption edges down to the K levels of the light elements C, O, and N, important in biology and chemistry. However, at the moment the magnetism community is most active in exploiting resonant effects. These basically arise from magnetic dichroism: the dependence of the absorption coefficient on the magnetisation in the material and the polarisation of the light.

The first soft X-ray magnetic scattering experiments have been performed on artificially ordered magnetic structures in the form of magnetic bi- and multilayers. Last year, it was shown that it is also possible to obtain information on magnetic domain structures in thin films. In this experiment [1], polarised X-rays were scattered off FePd thin films in which the magnetisation self-organises in so-called magnetic stripe domains (see inset). These structures act as a magnetic grating that produces well-defined satellites around the specular reflected beam. By varying the angle of incidence, it was shown that one can also obtain information on the domain structure

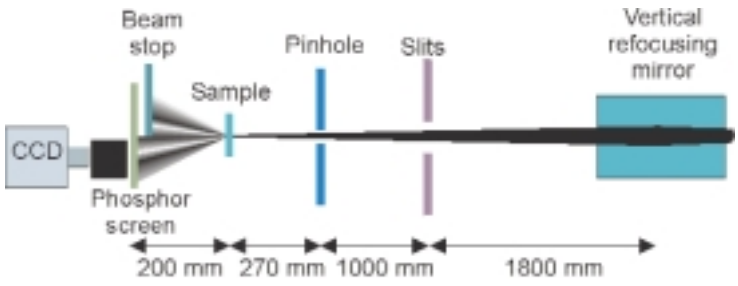

Fig. 1: Experimental layout. Note that the whole optical path from front end to scintillation screen is under ultra-high vacuum.

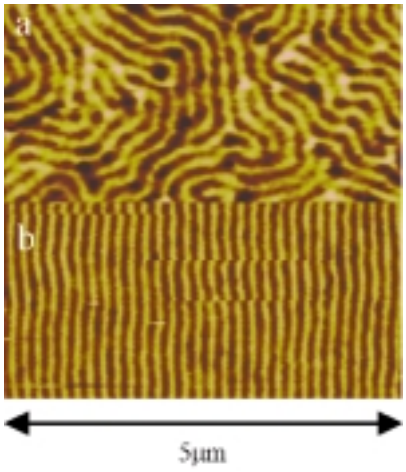

Fig. 2: (a) Magnetic force microscopy (MFM) image of the meandering magnetic stripe domains in a 35 nm thick film of $GdFe_2$. The width of the domains is 110 nm. (b) Parallel stripe domains obtained after saturation of a sample in an in-plane magnetic field applied along the stripe direction.

below the surface, which is very important since most domain imaging techniques only probe the magnetic profile of the fringe fields just outside the sample surface.

Recently, in a variant of these experiments on **ID12B** we have used a SAX-type transmission geometry, as shown in Figure 1. A 15 μm diameter beam was incident normally on a 35 nm thick film of amorphous $GdFe_2$ showing a pattern of 110 nm wide meandering magnetic stripe domains (Figure 2a.). Off-resonance, only the transmitted beam is observed. This changes radically when the energy of the beam is tuned to the Gd M_5 resonance (λ = 1.1 nm). Here the magnetic scattering cross-section is enhanced by orders of magnitude [2] and a clear first order and a much weaker third order (not shown) magnetic

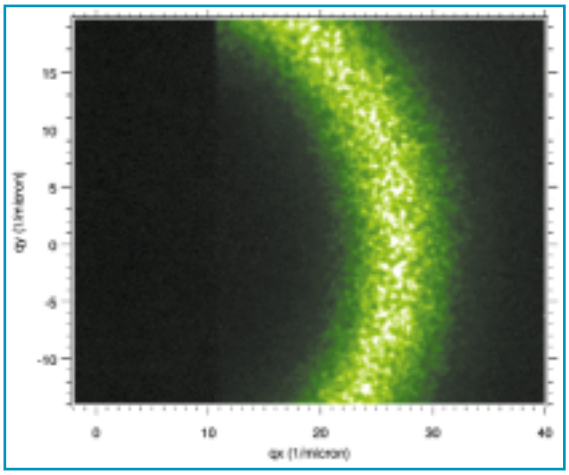

Fig. 3: Magnetic speckle observed on the first order magnetic diffraction ring in transmission from the sample described in Fig. 2a, illuminated by a 15 µm diameter beam of circularly polarised X-rays tuned to the Gd M_5 resonance at 1183.6 eV. A beam stop blocked the direct transmitted beam. The radius of the ring corresponds to a ~115 nm domain width.

diffraction ring appears (Figure 3). The total scattered intensity in the ring is 1.5 x 10^6 photons/s.

A closer look at Figure 3 reveals that the intensity in the ring has strong spatial fluctuations. These are static magnetic speckles, a result of the disordered magnetic structure in the scattering volume. Prior to this observation, magnetic speckles were reported on a Bragg diffracted peak of UAs [3]. Even though Figure 3 was recorded with non-optimised conditions, the speckle contrast is ~30%, indicating partial coherence with a coherence length of 5 μm. That one can do better is shown in Figure 4, which represents the Fraunhofer pattern of a 10 μm-diameter laser pinhole. It shows extremely regular diffraction rings up to the 24th order, implying nearly complete coherence. It was produced from the vertically convergent beam behind the vertical focusing mirror by collimating the beam with 300 x 500 μm slits, 1 m upstream from the pinhole (Figure 1). The total flux in this pattern is estimated at 1.3 x 10^7 photons/s.

As mentioned previously by Yakhou *et al.* [3], magnetic X-ray intensity fluctuation spectroscopy may be made possible by using such high fluxes. Probably the best chances for achieving this lie in the soft X-ray range, due to the inherently higher coherence length of soft X-ray undulators and the larger magnetic contributions to the scattering cross section. That being said, a large number of problems have to be surmounted. Primary concerns are the flux and the stability of the beamline. Hopefully the move of beamline ID12B to straight section ID8 will overcome these problems because it will then have a full length undulator with an estimated 10 times higher flux and a more stable optics layout. ■

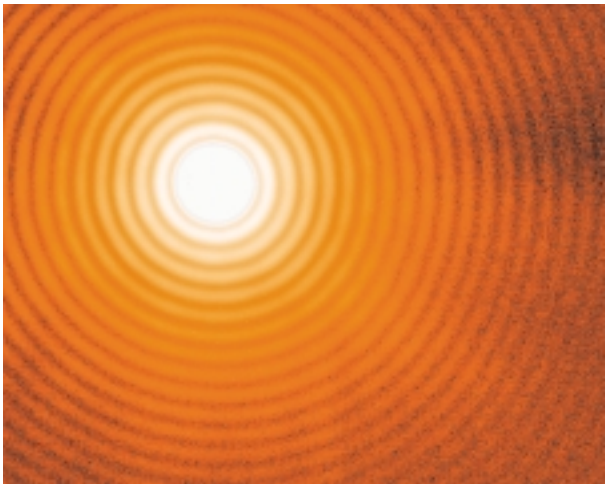

Fig. 4: Fraunhofer diffraction pattern from a 10 µm pinhole illuminated by a coherent beam of 1183.6 eV X-rays at ID12B. The total flux in this image is 1.3 10^7 photons/s with a 80 mA 16 bunch beam.

MAGNETIC DOMAINS IN THIN FILMS WITH A PERPENDICULAR MAGNETIC ANISOTROPY

Domains in magnetic thin films with a perpendicular magnetic anisotropy are the result of the competition between the magneto-static energy, which, to minimise the stray field, tends to an in-plane magnetised film (Figure 5a), and the perpendicular anisotropy, favouring an out-of-plane magnetisation (Figure 5b).
A configuration with alternating up and down domains (Figure 5c), reduces the stray field of the sample while most of the sample is perpendicularly magnetised, lowering the perpendicular anisotropy energy at the cost of creating domains walls [4]. Many different domain patterns are possible for the alternating up-down profile, for example the maze-like domain pattern and the perfect parallel stripes shown in Figure 2.

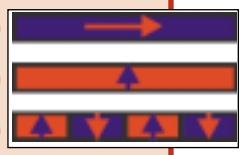

Fig. 5: Magnetisation profiles in a thin film, (a) uniform in-plane magnetisation, (b) uniform perpendicular magnetisation, (c) alternating up and down domains.

REFERENCES

[1] H.A. Dürr, E. Dudzik, S.S. Dhesi, J.B. Goedkoop, G. van der Laan, M. Belakhovsky, C. Mocuta, A. Marty, Y. Samson, Science, 284, 2166-2167 (1999).

[2] J.P. Hill, D.F. McMorrow, Acta Crystallogr., A52, 236-244 (1996).

[3] Yakhou et al., ESRF Newsletter, 32, 12-13 (2000).

[4] A. Huber and R. Schäfer in Magnetic Domains and references therein, Springer Verlag (1998); C. Kittel, Phys. Rev., 70, 965-971 (1946).

ACKNOWLEDGEMENTS

We thank the staff of ID12B and the authors of [1] for their help and contributions, and Otto Hopfner for technical assistance. This work is part of the research program of the Foundation for Fundamental Research on Matter (FOM) and was made possible by financial support from the Netherlands Organisation for Scientific Research (NWO).

First Observation of Molecular Vibrational Excitations of Water with Inelastic X-ray Scattering

C. Halcoussis[1], T. Abdul-Redah[2], H. Naumann[2], G. Monaco[1] and C.A. Chatzidimitriou-Dreismann[2]

1 ESRF, Experiments Division
2 I.N. Stranski Institute, Technical University of Berlin, Berlin (Germany)

The inelastic X-ray scattering (IXS) technique has been applied to the energy transfer regime of molecular vibrations of covalently bonded H atoms, ca. 0-500 meV. We have obtained, for the first time, convincing experimental evidence that IXS can be used for vibrational spectroscopy.

The ubiquitous condensed matter system called "liquid water" has always been in the focus of fundamental research. In particular, the manner in which it renders the earth fit as a habitat for life, and its involvement in life processes at all levels has inspired generations of researchers. Nowadays, it is widely known that most of the unique physicochemical properties of liquid water are intrinsically related to the huge amount of H-bonds, which determine its structure and dynamics from the macroscopic to the microscopic spatial and temporal scales. Additionally, the role of water in the formation and stabilisation of biologically significant structures is well known.

In the last few decades it has been recognised that quantum mechanical effects appear to play a dominant role in the proper microdynamical description of water due to the small mass of the hydrogen atom. Nowadays, modern spectroscopic techniques like neutron and X-ray scattering are indispensable for the study of matter in the mesoscopic and microscopic spatio-temporal domains. Extending the basic results obtained with inelastic neutron scattering, the recent development of the novel inelastic X-ray scattering (IXS) technique at a third generation synchrotron radiation source, the ESRF, has also led to a new interpretation of an important phenomenon in liquid water, i.e. a propagating "fast sound" collective mode at the mesoscopic scale [1].

The primary goal of our recent experiment (February 2000) at beamline **ID16** was to take the first measurement of the spectra of intramolecular vibrations (or, in other terms, localised vibrational excitations) using the IXS method. The OH stretching vibrational modes of water are about 400 meV. Before our experiment was performed, the possibility of observing such spectra had been questioned by many due to the very low intensity available at the spectral regime under consideration. Figure 1 shows the vibrational spectra of pure H_2O, pure D_2O and a H_2O-D_2O mixture with an equimolar H:D composition, i.e. H:D = 1:1. The accumulation time required for each of the spectra shown was about 40 hours. The spectra are presented as measured, i.e. no smoothing has been applied. The peaks due to the OH and OD stretching vibrational modes are clearly

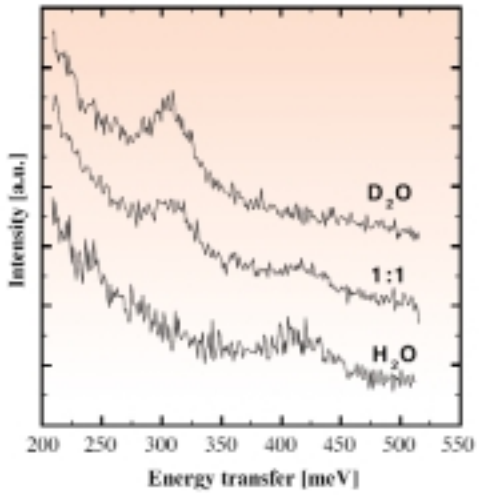

Fig. 1: The IXS spectra of the intramolecular OH and OD stretching modes of H_2O, D_2O, and a H_2O-D_2O mixture with an equimolar H:D composition (H:D = 1:1). The spectra are parallelly shifted, for illustration. Intensities are given in arbitrary units. (For the H_2O spectrum, a typical count rate at 400 meV was about 0.4 - 0.5 counts/s).

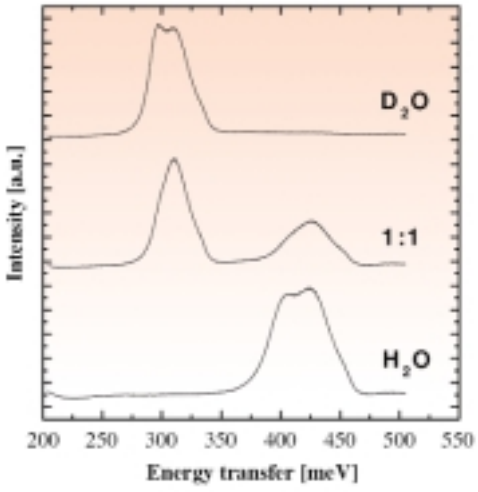

Fig. 2: The corresponding spectra of H_2O, D_2O, and the equimolar H_2O-D_2O mixture (H:D = 1:1) obtained with the conventional Raman light scattering technique (after standard data analysis). The spectra are parallelly shifted, for illustration. Intensities are given in arbitrary units. (Typical count rates at the maximum of the OH peaks were ca. 100 to 200 counts/s).

visible, and they are centred about 400 meV and 300 meV, respectively. These peaks are superimposed on the "long tail" of the much more intensive quasielastic peak. For the sake of visibility, the spectra are parallelly shifted. For the H_2O spectrum, a typical count rate at 400 meV was about 0.4 - 0.5 counts/second. The momentum transfer chosen in these experiments was 2.9 $Å^{-1}$. The incident energy was 13.8 keV. The spectral resolution used was about 12 meV. For comparison, the corresponding Raman light scattering spectra are shown in Figure 2. (An Argon-ion laser with excitation wavelength of 5140 Å was used. Typical count rates at the maximum of the OH peak were ca. 100 to 200 counts/second.) One can easily see that with both methods the same spectral positions of the OH and OD peaks were obtained. Obviously, the determination of the spectral peak shapes and widths of the IXS spectra require better counting statistics.

The second goal of our IXS experiment was to investigate the possibility of observing quantum entanglement (QE, cf. side panel) between the vibrational modes of liquid water. QE and/or Schrödinger's cat states of quantum particles play a dominant role in numerous present day investigations of fundamental (theoretical and experimental) physics. Moreover, articles about "quantum computer", "quantum cryptography" and "quantum teleportation" can be found even in rather popular journals; see for instance [2]. However, one conventionally expects that the observation of QE effects is impossible in condensed matter at room temperature, due to the extremely fast decoherence process [2,3] which destroys these quantum effects.

In our neutron Compton scattering (NCS) experiment on water and H_2O-D_2O mixtures [3] we have provided the first direct experimental evidence for QE between protons in water at room temperature. The NCS technique is characterised by a short scattering time (or interaction time of neutrons with protons) of about 1 femtosecond. The most surprising result was that, due to protonic QE, the cross-section density of H becomes reduced anomalously by up to 30%. In simple terms, QE seems to effectuate destructive quantum interference between protons, in the sub-femtosecond time scale [3]. Since OH oscillators contain protons, this striking NCS result indicates that the quantum dynamics of OH vibrations (and H-bonds), and the associated IXS spectra, could also be affected by protonic QE.

In future work, after further IXS data accumulation, we intend to determine the integral scattering intensities of the OH and OD peaks of the samples mentioned above (see Figure 1). If QE between vibrational degrees of freedom is present in water, then an anomalous change of the X-ray scattering cross-section density of the OH mode will be measurable. Concretely, the integral cross-section density of the OH mode of the H_2O-D_2O mixture would then be smaller (say, by ca. 10%) than that of the pure H_2O. In this case, one would observe the surprising effect that ca. 10% of the OH oscillators of the H_2O-D_2O mixture would become "invisible" to the X-rays. It may be noted that neutron scattering is due to the strong interaction, whereas IXS is due to the electromagnetic interaction. Thus it will be interesting to compare the anomalies found with NCS [3] with the associated IXS results. If successful, our IXS experiment on water will reveal novel characteristics of short-time quantum dynamics of protons (and H-bonds) in condensed matter.

References

[1] G. Ruocco, F. Sette, U. Bergmann, M. Krisch, C. Masciovecchio, V. Mazzacurati, G. Signorelli, R. Verbeni, Nature, 379, 521-523 (1995).

[2] A. Zeilinger, Quantum teleportation, Scientific American, 282 (no.4), 32-41, (April 2000).

[3] C. A. Chatzidimitriou-Dreismann, T. Abdul-Redah, R. M. F. Streffer, J. Mayers, Phys. Rev. Lett. 79, 2839-2842 (1997).

Quantum entanglement (QE) of two systems

Consider two dice (say, A and B) which are rolled. As conventionally assumed, each dice on its own should be fair and yield random results. The two outcomes of a throw with the two dice are then completely uncorrelated.

Of course, dice are classical objects. Nevertheless let us now make the (fictitious) assumption that the two dice are quantum objects. After rolling of the dice pair, its wavefunction, say Ψ_{AB}, can be constructed with the aid of the "single-dice" wavefunctions $\Psi_A(i)$ and $\Psi_B(j)$, where i and j are possible outcomes, that is, natural numbers from 1 to 6. There are many different forms of Ψ_{AB} that are permissible according to quantum theory. Some of them – in fact, the majority of them – appear to have completely counter-intuitive properties. Here let us give a particular example of such a state (which is adapted from Ref. [2]). E.g., for the specific case of "equal outcomes", the following dice-pair wavefunction (before an actual measurement of the outcomes; see below) is permissible according to the fundamental Superposition Principle of quantum mechanics (see any textbook):

$$\Psi_{AB} = \text{const.} * [\Psi_A(1) * \Psi_B(1) + \Psi_A(2) * \Psi_B(2) + ... + \Psi_A(6) * \Psi_B(6)] \quad (1)$$

The physical meaning of this Ψ_{AB} may be described as follows: The outcomes of both dice A and B are equal to 1 and, at the same time, they are equal to 2, ..., and, at the same time, they are equal to 6. This specific quantum state has no classical analogue and thus it is completely counter-intuitive.

An actual measurement of the two outcomes "reduces" Ψ_{AB} to another wavefunction, say Φ_{AB}. E.g., if one actually measures a "double 5", then the wavefunction of the dice pair after the measurement is

$$\Phi_{AB} = \Psi_A(5) * \Psi_B(5) \quad (2)$$

[This is according to the standard theory of measurement; in technical terms, applying the von Neumann projection postulate.] Clearly, in contrast to (1), the wavefunction (2) has a classical analogue.

A pair of quantum systems being in a quantum state like (1) – but not like (2) – is called entangled. Quantum states like (1) are also called Schrödinger's cat states, Einstein-Podolsky-Rosen states, etc. Nowadays, entangled pairs of quantum objects (e.g., photons or ions, which must be very well isolated from their environment) can be produced in the laboratory; cf. [2].

Pressure-induced Landau-type Transition in Stishovite

D. Andrault[1], G. Fiquet[2], F. Guyot[2], M. Hanfland[3]

1 Laboratoire des Géomatériaux, Institut de Physique du Globe, Paris (France)
2 Laboratoire de Minéralogie-Cristallographie, Université Paris VII and IPGP, Paris (France)
3 ESRF, Experiments Division

Rietveld structural analysis of SiO_2-stishovite could be performed up to 120 GPa by angle-dispersive X-ray diffraction in a YAG-laser heated diamond anvil cell. At 54 GPa, a second-order pressure-induced lattice modification occurs. Above this pressure, the $CaCl_2$-type SiO_2 compresses without additional decrease of the shortest known O-O bond found in stishovite.

There is no close-packed compact ionic arrangement for metal dioxides. The most common dense form of XO_2 compounds (where X is Si, Ti, Ge,...) is rutile, in which the oxygen sublattice can be seen as largely distorted face centered cubic, and where only one of the two octahedral sites is filled by silicon (Figure 1). There are several other dense forms for the XO_2 compounds, because comparable energies are found for slightly different octahedral inter-links. For example, six polymorphs have been reported for PbO_2, between ambient pressure and 47 GPa [1]. The sequence of the SiO_2 phase transformations down to the core-mantle boundary (CMB) of the Earth needed further analysis because it can affect the lower mantle composition through a possible breakdown of the major lower mantle mineral, the $(Mg,Fe)(Al,Si)O_3$ perovskite, into a mixture of stishovite and magnesiowustite.

Synthetic crystals of quartz were finely ground, mixed with platinum black, and loaded in a membrane-type diamond anvil cell. After each pressure increase, the sample chamber was slowly scanned by the infrared radiation of a multimode regulated YAG-laser. This laser-annealing technique is a very efficient method of relaxing the sample stress and leads to a quasi-hydrostatic pressure in the pressure chamber, improving the quality of the X-ray diffraction spectra [2,3]. Angle-dispersive X-ray diffraction spectra were recorded at the **ID9** beamline. A water-cooled Si (111) bent Laue

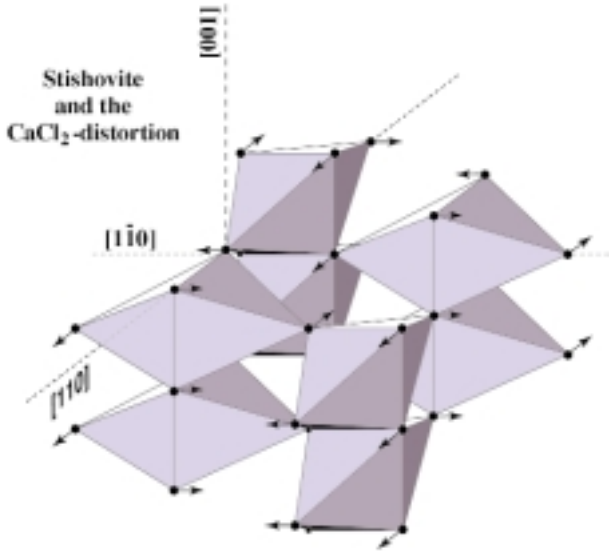

Fig. 1: Dense atomic arrangement for silica. One half of the octahedral sites of the oxygen sublattice are filled by Si atoms. SiO_6 octahedra show 4 equatorial and 2 polar Si-O bonds. The $CaCl_2$-distortion occurs when oxygen escapes from the diagonal of the (a,b) plane, thus changing symmetry from tetragonal to orthorhombic.

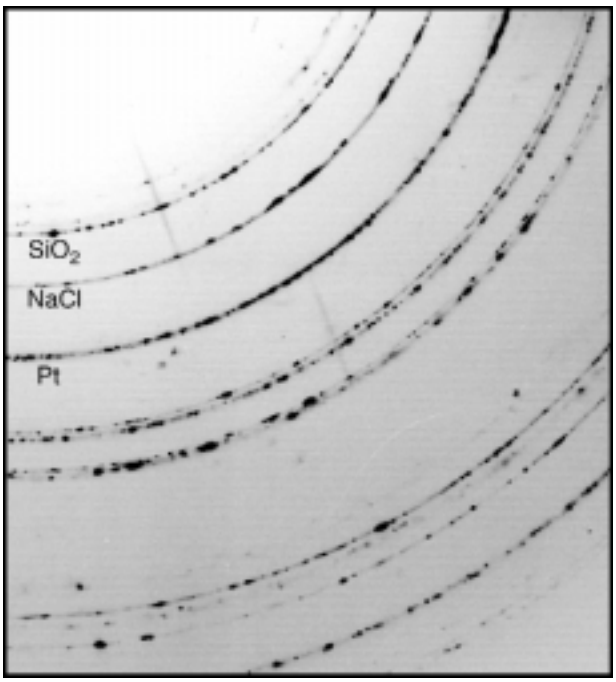

Fig. 2: Typical two dimensional diffraction pattern recorded on a mixture of SiO_2-stishovite, NaCl pressure transmitting medium, and Pt YAG-absorber. This pattern was recorded at 11.7 GPa, after laser heating to about 2200 K in the diamond anvil cell.

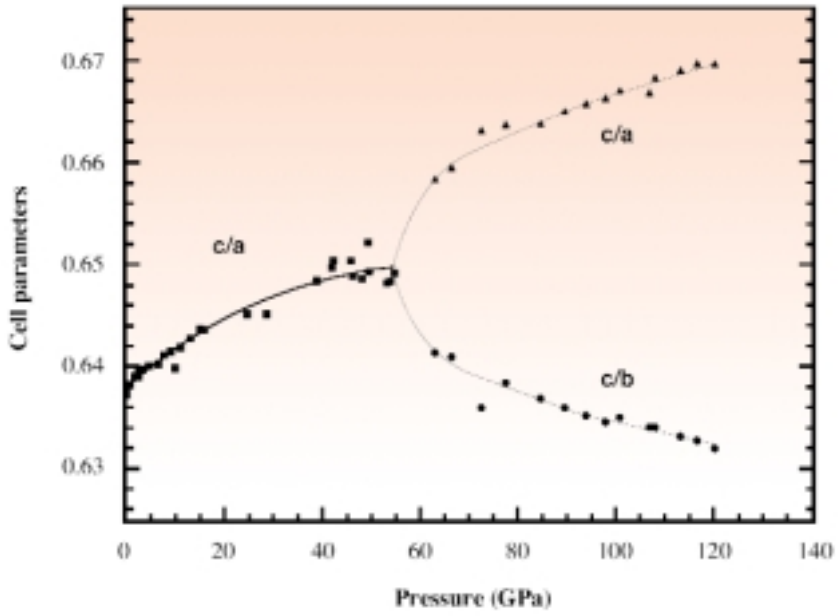

Fig. 3: Pressure evolution of the unit cell parameters showing a rapid increase in the difference between a and b axes above 54 GPa. The evolution with pressure of the (a-b)/a order parameter indicates a classical Landau-type evolution, with the $CaCl_2$-form being the lower entropy polymorph.

monochromator was used to produce a bright monochromatic X-ray beam at a wavelength of 0.4561 Å. Vertical and horizontal focusing was achieved with a spherical mirror and a monochromator, respectively. The X-ray flux on a 15*15 μm spot allowed acquisition on an imaging plate in about 10 minutes [4]. The two-dimensional images (Figure 2) were integrated using the program Fit2d. Lebail and Rietveld profile refinements were applied to all diffraction patterns to extract cell parameters and volumes for SiO_2 and platinum, and to compare experimental intensities with those calculated for different structural models of SiO_2.

Analysis of the X-ray diffraction spectra indicates that the sample consists of a mixture of platinum and stishovite up to 53.2 GPa. The spectrum recorded at 54.8 GPa shows slight modifications related to the onset of a transformation from stishovite to a $CaCl_2$-distortion of stishovite. At 62.4 GPa, the diffraction peaks located at around 1.45 and 1.78 Å become doublets, which the stishovite model fails to explain. Instead, the modelled spectrum of the $CaCl_2$-distortion of stishovite fits the experimental profile. The occurrence of the $CaCl_2$-polymorph at about this pressure agrees with previous experimental reports using either X-ray diffraction [5] or Raman spectroscopy [6]. It also agrees with *ab-initio* structure simulations that proposed a $CaCl_2$-distortion, but is in disagreement with other experimental or theoretical studies that proposed the occurrence of a post-$CaCl_2$ polymorph at pressures below 120 GPa, at the pressure conditions of the Earth's lower mantle.

Evolution of c/a and c/b cell parameter ratios (Figure 3) clearly shows the stishovite to $CaCl_2$-form transition: there is an increase in the $CaCl_2$-distortion with increasing pressure up to 120 GPa. The rapid modification of the a and b cell parameters above 54 GPa is achieved by a rapid rotation of the SiO_6 octahedra in the (a,b) plane, as supported by the pressure evolution of the (x,y,0) oxygen coordinates. We note a change in the pressure evolution of the shortest O-O distance above the transition pressure. In the $CaCl_2$-structure, the compression occurs without further decrease in this shortest O-O distance. Instead, the other O-O distances diminish toward a comparable value, and consequently the oxygen sublattice becomes more symmetrical.

The pressure evolution of the a and b cell parameters is similar to that usually found for a Landau-type temperature-induced transition. Using a standard type of representation for such a transition with the (a-b)/a ratio as an order parameter, results indicate that the $CaCl_2$-form is the lower entropy polymorph. Therefore, the $CaCl_2$-form may be the low-temperature polymorph of stishovite. This gives weight to the argument for a positive slope of the boundary between the two silica polymorphs in a P-T diagram. The critical temperature of the phase transition (Tc(P)) would reach T = 300 K, when pressure reaches 54 GPa. This means that while further compressing silica at room temperature (T_{exp}) above 54 GPa we increase the gap between the experimental and critical temperatures (the gap is T_c-T_{exp}). For such a second order transition, an increase in (T_c-T_{exp}) explains the increase of the $CaCl_2$-distortion that was observed.

We observed a continuous increase in the SiO_2 density up to pressures found at the Earth's CMB, because the phase transformation to the $CaCl_2$ polymorph do not involve noticeable modification of volume or bulk modulus. From these new data we calculate a positive ΔV for the $MgSiO_3$ => MgO + SiO_2 breakdown reaction at all pressures. Therefore, the silicate perovskite is denser than a mixture of its oxides down to the CMB. **Consequently, the proposal that free silica could occur in the Earth's lower mantle is not supported by the present data, as long as an excess of magnesiowustite (Mg,Fe)O is believed to be present in the lower mantle.**

References

[1] J. Haines, J.-M. Léger, O. Schulte, J. Phys. Condens. Matter, 8, 1631 (1996).

[2] G. Fiquet, D. Andrault, J.-P. Itié, Ph. Gillet, P. Richet, Phys. Earth Planet. Int., 95, 1 (1996).

[3] D. Andrault, G. Fiquet, M. Kunz, F. Visocekas, D. Häusermann, Science, 278, 831 (1997).

[4] D. Häusermann, M. Hanfland, High Pressure Res., 14, 223 (1996).

[5] Y. Tsuchida and T. Yagi, Nature, 340, 217 (1989).

[6] J. K. Kingma, R. E. Cohen, R. J. Hemley, H. K. Mao, Nature, 374, 243 (1995).

Small-angle X-ray Diffraction Study of Monoolein under Pressure: Stability and Energetics of Pn3m and Ia3d Bicontinuous Cubic Phases

P. Mariani[1], M. Pisani[1], C. Ferrero[2], A. Cunsolo[2] and T. Narayanan[2*]

1 Istituto di Scienze Fisiche and INFM, Università di Ancona (Italy)
2 ESRF, Experiments Division
* Corresponding author

A bicontinuous cubic liquid crystalline phase is one of the most fascinating structures exhibited by water/amphiphile systems. Not only do the structure and dynamics of these cubic phases make them attractive as model soft matter systems, but they also have many practical applications. Small-angle X-ray scattering can reveal the symmetry as well as the topology of these structures.

Lipids are natural examples of amphiphilic molecules having a polar head and a non-polar tail. Because of the hydrophobic character of the large nonpolar tail, and other factors such as packing and steric constraints, van der Waals and electrostatic interactions, these molecules exhibit a variety of self-assembled states when mixed with water. Which state predominates depends on the concentration and thermodynamic parameters such as temperature and pressure. In neutral lipids, the polar head group bears no net charge under biological pH. Monooleoylglycol (monoolein) is one such lipid, which is well known for its mesomorphism in the hydrated state. It is a workhorse lipid involved in fat digestion. On the mesoscopic scale, monoolein molecules in water organise into a wide variety of structures of which bicontinuous cubic phases are well known. These cubic phases have found application in the crystallisation of a variety of bacterial membrane proteins. Understanding the relationship between microstructure and phase stability is important in the study of their biological function. The stability of bicontinuous cubic phases and the ability of a lipid membrane to bend are governed by the bilayer elastic curvature energy.

At normal pressures, the monoolein and water mixture shows a variety of lyotropic phases. These include a lamellar phase (L_α) in which molecules assemble into stacked sheets (as shown in Figure 1a), an inverted hexagonal phase H_{II} consisting of cylindrical structural elements packed on a 2-D hexagonal lattice, and two inverted cubic phases with space group symmetries Pn3m and Ia3d [1,2]. As depicted in Figure 1, the cubic structures are formed by mid-planes of bilayers satisfying the condition for periodic minimal surface (mean curvature $\rightarrow 0$) [3,4]. Consequently, this system is suitable for testing the proposed curvature free energy model of lyotropic phases [3].

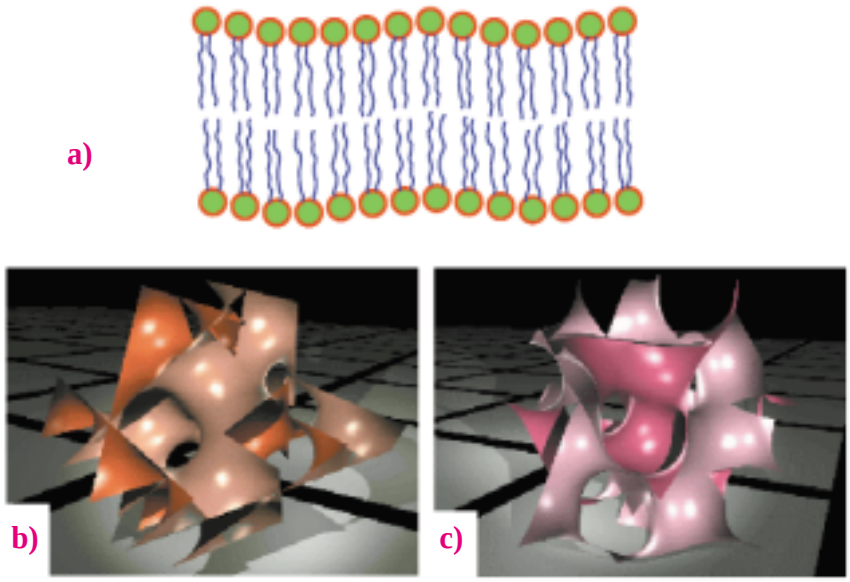

Fig. 1: (a) Schematic view of the cross-section of a lipid bilayer showing the hydrophilic head and hydrophobic tail of the lipid molecules. Computed periodic minimal surfaces corresponding to Pn3m (b) and Ia3d (c) cubic symmetries, respectively (courtesy of S. Hyde and S. Ramsden, Australian National University). In (b) and (c) each of the triply periodic minimal surfaces is formed by the lipid bilayer.

Hydrostatic pressure can be used to influence the structural properties and then to obtain an extended description of the phase behaviour, stability and energetics of cubic phases. Small-angle X-ray diffraction is a powerful tool for elucidation of the symmetry as well as the topology of these structures. Measurements were performed on the **ID2** beamline at the ESRF. Monoolein

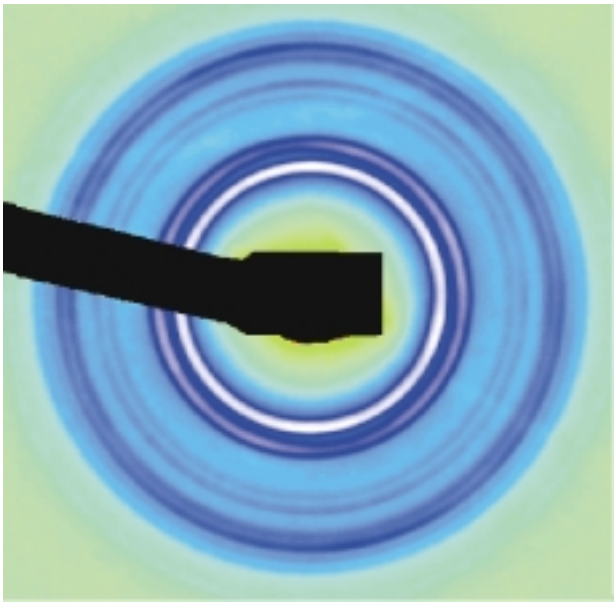

Fig. 2: Typical 2-D diffraction patterns from a cubic Ia3d phase at a pressure of 1.1 kbar and 28 wt.% of water.

samples were studied at different degrees of hydration (water content) as a function of pressure up to 3 kbar. A typical 2-D diffraction pattern from an Ia3d cubic phase is shown in Figure 2. Typical, azimuthally-averaged intensities as a function of scattering vector s (= $2/\lambda \sin\theta$) at different pressures are depicted in Figure 3. Results show that the pressure induces a transition from the Ia3d cubic to the lamellar L_α phase and then to the lamellar crystalline phase for a 30% hydrated sample. In the more hydrated samples, a cubic-to-cubic phase transition (Pn3m to Ia3d) was observed. The crystalline phase is the only one that survives above 3 kbar.

While the crystalline phase is found to be incompressible, the unit cell dimensions of the cubic and the lamellar L_α phases increase as a function of pressure. The monolayer thickness, the cross-sectional area per molecule, and the mean and gaussian curvature [3], as a function of pressure and composition derived from these data, are summarised in Figure 4. The observed behaviour clearly indicates that the pressure induces a continuous change in the shape of monoolein molecules. In the cubic phases, these changes imply the stretching of the hydrocarbon chains and the consequent reduction of their cross-sectional area, resulting in the decrease in the mean curvature at the polar/apolar interface. These deformations are clearly involved in the associated curvature elastic

Fig. 3: Azimuthally averaged diffraction patterns at different pressures for a sample of 30 wt. % water.

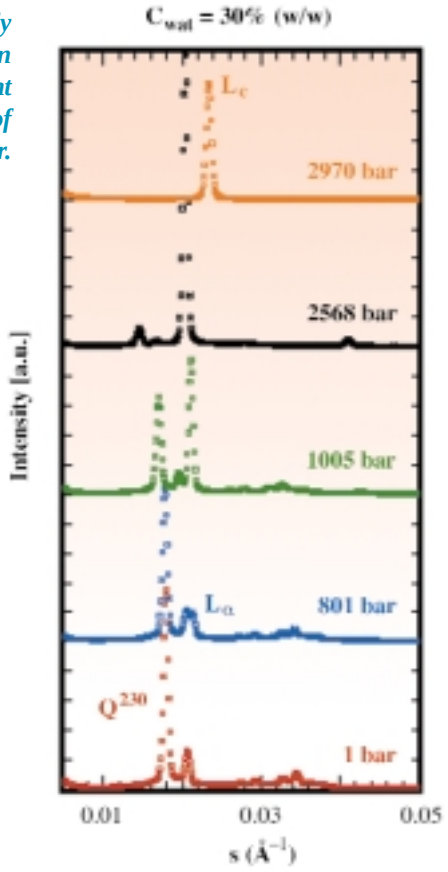

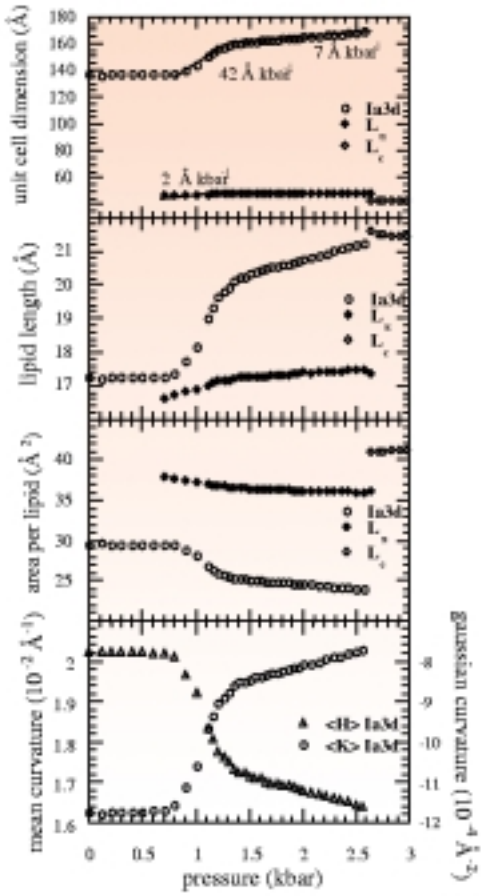

Fig. 4: Structural parameters deduced from the diffraction data as a function of pressure for a sample containing 30 wt.% of water.

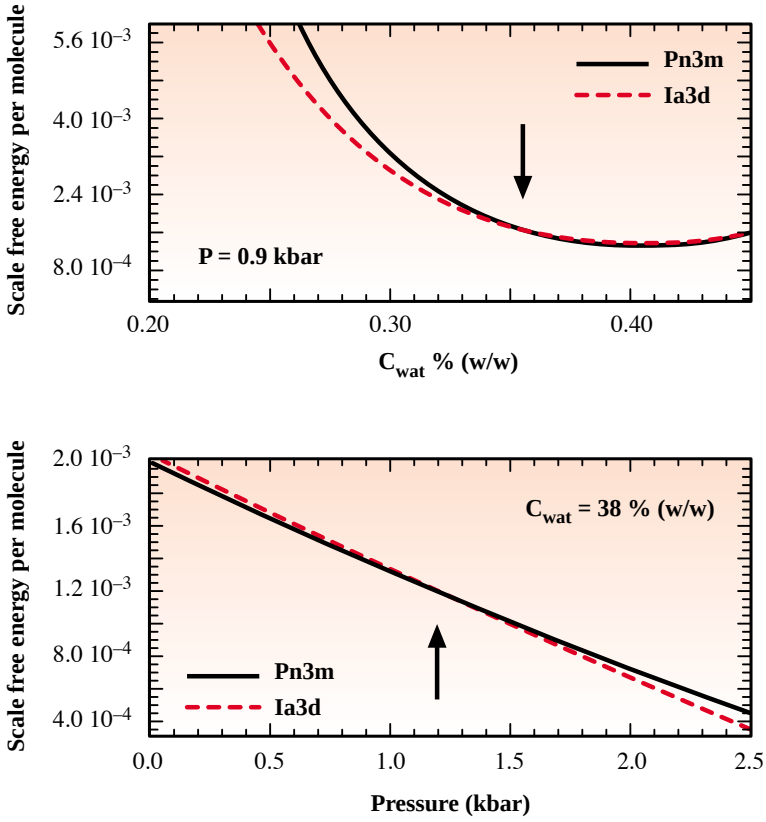

Fig. 5: Scaled free energy for the Pn3m and the Ia3d cubic phases as a function of concentration at constant pressure (P = 0.9 kbar) and as a function of pressure at constant concentration (38% w/w of water).

energy contributions to the cubic phase free energy which explains the observed phase behaviour.

Starting from the Helfrich description [3,5] for the curvature elastic energy, the ratio of the monolayer gaussian bending constant to mean-curvature bending constant k_G/k and the spontaneous curvature H_0 (the curvature that the monolayer would assume if it were free from all other constraints) were determined in the Pn3m and Ia3d cubic phases by a numerical fit of structural data obtained at different pressures. The pressure dependence of the spontaneous curvature and of the ratio k_G/k have been determined for the first time. Despite ignoring (or assuming only a minimal change across the phase transition at constant pressure) the chain packing and other contributions like interlamellar interactions, the curvature model provides the proper location and stability of each cubic phases with respect to the others, both as a function of pressure and concentration. For the sake of illustration, the recalculated free energy of Pn3m and Ia3d cubic phases as a function of concentration at constant pressure and as a function of pressure at constant concentration are shown in Figure 5. The arrow indicates the point at which the phase transition was observed experimentally. The good agreement demonstrates how well this type of experiment can provide a quantitative test of theories on stability and energetic of lyotropic phases. ■

REFERENCES

[1] H. Chung, M. Caffrey, Nature, 386, 224-226 (1994).

[2] P. Mariani, B. Paci, P. Bosecke, C. Ferrero, M. Lorenzen, R. Caciuffo, Phys. Rev. E, 54, 5840-5843 (1996).

[3] W. Helfrich, J. Phys.: Condens. Matter, 6, A79-A92 (1994).

[4] C. Toprakcioglu, in Theoretical Challenges in the Dynamics of Complex Fluids, ed: T. McLeish, Kluwer Academic, p 235 (1997).

[5] R.H. Templer, D.C. Turner, P. Harper, J.M. Seddon, J. Phys. II (France), 5, 1053-1065 (1955).

ACKNOWLEDGEMENTS

The ESRF chemistry laboratory (H. Müller and co-workers) is acknowledged for the synthesis of monoolein compound.

Generation of Short Pulses of Hydroxyl Radicals by Synchrotron Radiation for Time-resolved Hydroxyl Radical Footprinting

M. Roessle[1], E. Zaychikov[1], L. Denissova[1], M. Wulff[2], F. Schotte[2], M. Hanfland[2], B. Sclavi[3], C. Badaut[3], M. Buckle[3] and H. Heumann[1]

1 Max-Planck-Insitut für Biochemie, Martinsried (Germany)
2 ESRF
3 Institute Pasteur, Paris (France)

Short pulses of hydroxyl radicals can be generated by synchrotron radiation and used to follow biological processes at time intervals on the millisecond scale.

A key process of the cell is the transcription of the genetic information encoded in the DNA. This process is facilitated by the enzyme DNA-dependent RNA polymerase (RNAP), which moves along the DNA "reading" the DNA sequence and synthesising a base-complementary RNA. We intend to use hydroxyl radicals (OH•) in order to follow the movement of RNAP on the DNA in the millisecond range. Hydroxyl radicals cleave the DNA at those regions which are not covered by the RNAP. Due to the ionising property of the X-ray beam, high-intensity X-ray pulses can be used to produce short hydroxyl radical pulses which can cleave the DNA in the same manner as chemically generated hydroxyl radicals (Figure 1a).

The DNA is cleaved without significant base specificity (Figure 1b) by interaction of the hydroxyl radicals with the sugar moiety. Those regions on the DNA that interact with the protein are precluded from hydroxyl radical attack and appear in the gel electrophoretic pattern as windows (footprints) in the otherwise regular cleavage pattern (Figure 2). The cleavage pattern is visualised by autoradiography of the radioactively-labelled fragments which are electrophoretically separated – a procedure similar to DNA sequencing.

Hydroxyl radicals are routinely generated chemically by the Fenton reaction and are used for probing protein-DNA contacts. The rate-limiting step in this footprint reaction is the production of hydroxyl radicals. In the Fenton reaction the rate of chemically produced radicals is to low for fast footprinting. The integral amount of radicals for sufficient cleavage is reached after several seconds. Therefore, the time interval for subsequent footprints is limited to 20 seconds. Using the white beam of the X-ray synchrotron spectrum at ESRF's **ID9** beamline, it is possible to generate short pulses of OH• which enables footprinting at 10 millisecond intervals by increasing the rate of Hydroxyl radical production by a factor of 10^4.

Figure 2b shows a schematic footprint of RNA polymerase bound specifically to

Fig. 1: a) Production of hydroxyl radicals (OH•) by ionising radiation, b) Cleavage reaction of the DNA-backbone after hydrogen abstraction at the C4'-atom by the electrophilic, highly reactive hydroxyl radical.

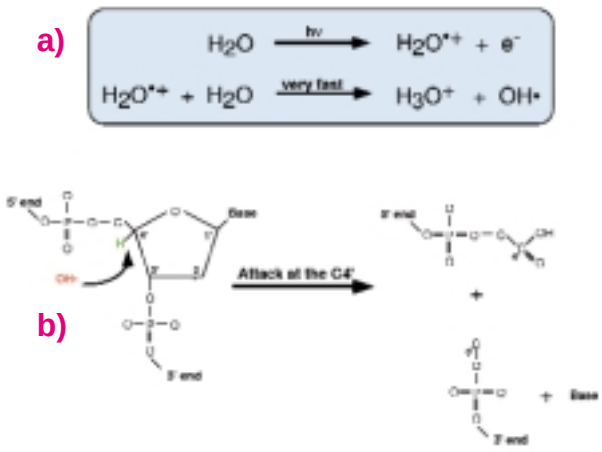

Fig. 2: Scheme of DNA-footprinting. a) The bound protein covers regions on the DNA and protects them from cleavage, b) This protected and therefore uncleaved region remains as missing bands in the cleavage pattern on the autoradiographic gel.

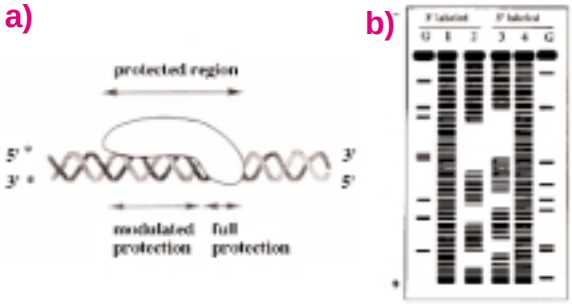

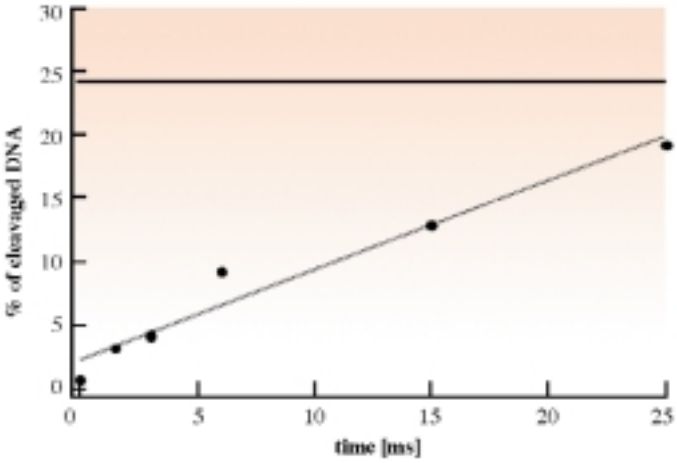

Fig. 3: Linear increase in cleavage with exposure time; the solid line indicates the percentage of cleavage using chemically generated hydroxyl radicals after a reaction time of 1 minute.

its cognate DNA fragment. The following information can be extracted from the hydroxyl radical footprinting patterns:

- The size of the DNA region interacting with the protein, which is obtained from the positions of the windows.
- The mode of interaction, which can be derived from the variation of the intensity of the bands within the interacting region. Protection of both strands indicates that the protein wraps around the DNA, whereas a window at both strands shifted by 10 bases indicates protein binding towards one side of the DNA.

In order to obtain quantitative data about the interaction of DNA and protein, the exposure time has to be adjusted in such a way that not more than 10 - 20% of the DNA molecules are cut. A simple criterion for the quality of the cleavage procedure is a linear increase in the band intensity with the exposure time. This linearity is demonstrated for our cleavage studies in Figure 3.

Cleavage by hydroxyl radicals occurs not only in the DNA but also in the protein. However, this does not interfere with the interpretation of the footprinting data, since the DNA is cleaved much more efficiently than the protein due to its higher sensitivity towards the hydroxyl radical. Only the DNA fragments which are cleaved by hydroxyl radicals produce the characteristic band pattern on the electrophoresis gel. Direct strain breaks of the DNA-helix due to radiation damage would produce DNA fragments of every size and lead to a strong background on the gel. Therefore the exposure time has to be adjusted to obtain good cleavage with minimal radiation damage.

In order to follow the movement of the RNA polymerase along the DNA, the footprints have to be determined in the millisecond time range. One prerequisite is rapid mixing of the components, which is achieved by a fast mixing device having a dead-time below 20 ms. The machine consists of a system of syringes and produces a continuous flow of mixed sample through the irradiated capillary. A stepping motor controls the flow-rate, permitting a minimal exposure time of 0.5 ms/μl. This device was installed at the ID9 beamline using the wiggler (gap at 30 mm) without any beamline optics. The sample was irradiated with a 2.5 x 1 mm^2 beam using a quartz capillary (OD 1 mm; walls 0.01 mm). Damage to the capillary was avoided by using glassy carbon and aluminium attenuators.

Figure 4 shows the first footprint of RNA polymerase obtained by X-ray synchrotron radiation in 10 ms. On the gel, the protected regions are visible as areas with less pronounced or missing bands (Figure 4a). The larger region indicates the full protection of the DNA by the protein and the smaller regions above, separated by windows of ~10 base-pairs, the half protection of the DNA. Further analysis of the pattern is done by integrating the profile of the pattern (Figure 4b). In the profile the protected regions, compared to unbound DNA are shown. The pattern is compatible with that obtained by chemically generated OH-radicals after 20 s.

Potential applications of the footprinting technique include the analysis of the structural rearrangements of RNA polymerase and DNA during formation of the transcription competent initiation complex. During formation of this complex at least three different intermediate complexes are transiently formed, namely the closed complex,

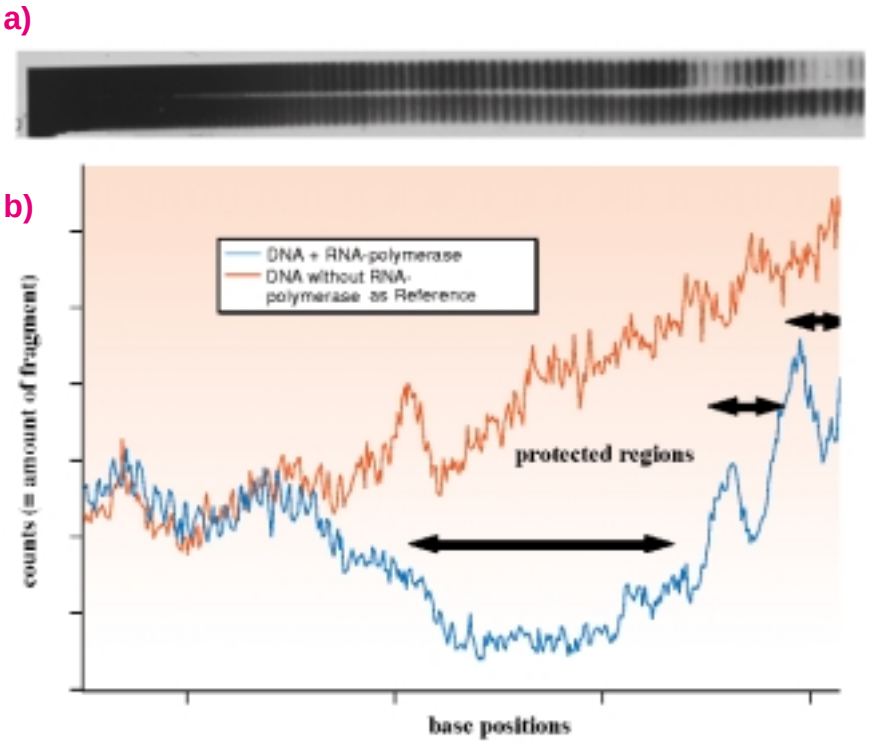

Fig. 4: Footprint of the RNA-polymerase on the DNA. a) Experimental data: Upper pattern RNA-polymerase + DNA; lower pattern DNA alone, as reference, b) Profile analysis of the cleavage pattern from a).

the intermediate complex and the transcription competent open complex. These intermediates are characterised by kinetic studies and by chemical footprinting. The later required lowering of the temperature in order to "freeze" the intermediate complexes. Fast Footprinting by synchrotron-generated hydroxyl radical pulses would allow direct structural characterisation of the intermediates.

Another fascinating application of this technique would be the analysis of the formation of initiation complexes which are controlled by helper proteins such as the Fis-protein. These helper proteins play an important role for the control of gene expression not only in bacteria but also in eucaryotic cells.

A related project which could also be tackled by Fast Footprinting is the analysis of the translocation of RNA polymerase along DNA during the transcription process in real time – a "cinematographic" analysis. This process is probably not monotonous and does not occur in parallel with incorporation of each nucleotide into the RNA. The latter process occurs approximately every 50 - 500 milliseconds. In order to follow this process in real time, Fast Footprinting using synchrotron-generated OH-radicals is presently the only direct approach to follow the movement of the enzyme on the DNA. This translocation process recently gained special attention, since RNA polymerase can be considered as a highly processive linear molecular motor.

ACKNOWLEDGEMENTS

We thank the DFG for support.

X-ray Imaging with Sub-100 nm Spatial Resolution at 4 keV

B. Kaulich, R. Barrett, M. Salomé, S. Oestreich and J. Susini

ESRF, Experiments Division

The ID21 transmission X-ray microscope is an instrument which, in addition to offering the opportunity for sub-100 nm imaging with exposure times in the second and minute range, extends the imaging technique to spectro-microscopy applications thanks to the specific design of its monochromator.

A transmission X-ray microscope (TXM) for the photon energy range of 3-7 keV has been installed on the ID21 beamline. The optical scheme of the TXM (Figure 1) is analogous to that of a visible light microscope where the incident radiation is condensed onto the object and a magnified image of the sample is formed by an objective lens onto a spatially resolving detector. Zone plates are used as the condenser and imaging objective optics [1]. When compared to a TXM for soft X-rays, the major difference is that the setup for spectro-microscopy applications includes a Si monochromator with an energy resolution of about 10^{-7} [2]. The other difference is a consequence of the low emittance of insertion device sources at third generation synchrotrons; the low numerical aperture illumination makes it difficult to use a condenser as the unique beam-condensing element. To overcome this limitation, a rotating two-mirror assembly can be introduced into the condenser system to match the numerical aperture between the condenser and the imaging objective and to generate quasi-incoherent illumination [3,4]. The strategy adopted for the ID21 TXM was to favour mechanical stability for sub-100 nm spatial resolution imaging by keeping the design compact. The microscope's construction is highly modular and readily adaptable to different imaging modes. This approach allows sufficient space to be reserved for a variety of sample stage environments and, in particular, will allow later implementation of specialised stages for tomographic and cryogenic imaging.

To illustrate the imaging capabilities of the microscope, a customised test object was manufactured. The 400 nm-thick Au object was a variable line-spacing grating with line widths from about a micrometre down to 85 nm. The grating was imaged using an Au micro-zone plate with an outermost zone width of 70 nm. Both test object and micro-zone plate were generated at the Institute for X-ray Physics (IRP), Goettingen, Germany [5]. The 1 mm-diameter Au condenser zone plate was fabricated at the IESS/CNR, Rome, Italy [6] and has a diffraction efficiency of 19%. Figure 2 shows an absorption contrast X -ray image of the Au grating which was acquired at a photon energy of 4 keV with an exposure time of 1 s. The smallest lines of 85 nm can clearly be resolved with good contrast - this is the best performance reported for such a microscope at these energies.

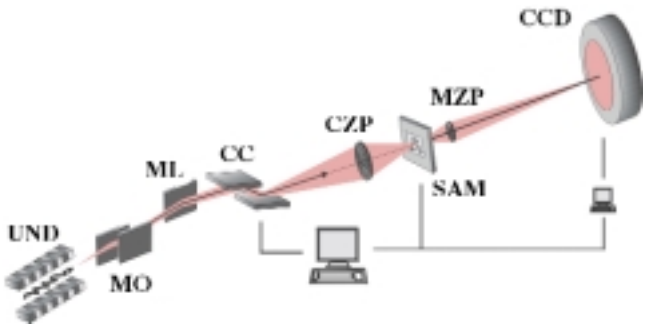

Fig. 1: Optical scheme of the transmission X-ray microscope at the ID21 beamline with the low bandpass filtering double mirror (MO), the beam-steering multilayer (ML), a channel-cut monochromator (CC), a large diameter zone plate (CZP) which condenses the beam onto the sample (SAM), and a micro zone plate (MZP) which produces a magnified image at the detector (CCD).

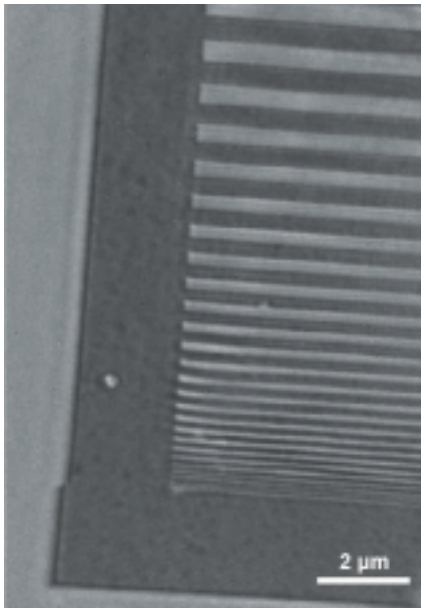

Fig. 2: High spatial resolution X-ray image of an Au test grating with varying line width from a few micrometres down to 85 nm. The image was taken at a photon energy of 4 keV, the exposure time was 1 s. The smallest structures of 85 nm can clearly be resolved with good contrast.

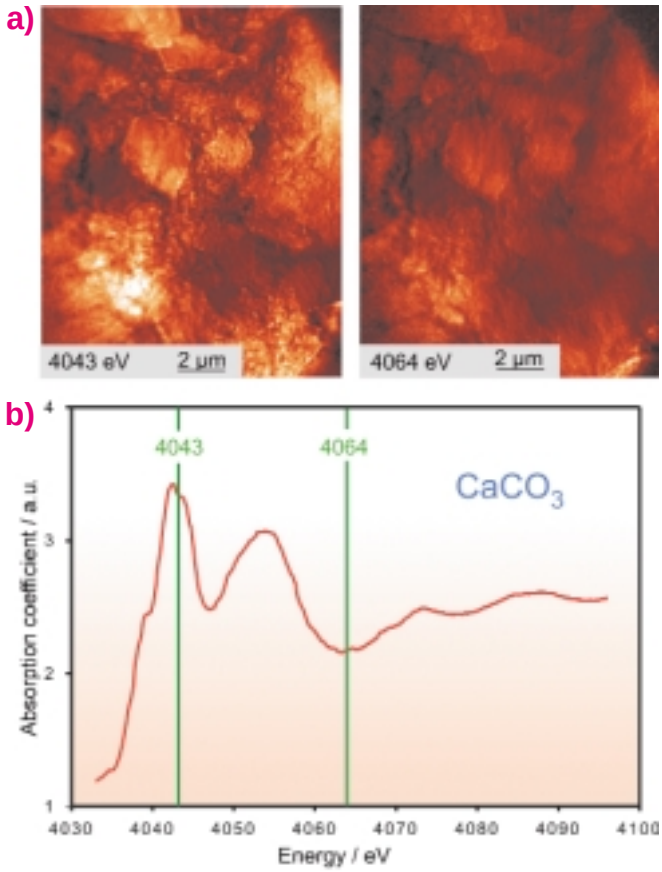

Fig. 3: X-ray spectro-microscopy: (a) Two sections of an energy stack of X-ray images of a concrete sample after the Ca K-edge, (b) the $CaCO_3$ spectrum recovered from a region of interest through the image stack.

The feasibility of spectro-microscopy was demonstrated by imaging concrete samples. A series of a hundred images was taken across the Ca K-edge (4038 eV), with energy steps of 0.6 eV and 30 s exposure time. The flat-field corrected images were aligned and organised in a three-dimensional array or energy stack, allowing quick access to the spectrum of any region of interest in the image (Figure 3).

The microscope is now being used for a wide variety of applications. It is suitable for the use of complementary imaging modes like absorption, Zernike phase or interference contrast. It offers the possibility of near-edge absorption studies for elemental mapping and analysis of the chemical states of the sample with sub-100 nm spatial resolution within the 3-7 keV energy range.

References

[1] B. Kaulich, T. Wilhein, S. Oestreich, E. Di Fabrizio, M. Gentili, P. Charalambous, M. Salome, R. Barrett, J. Susini, Appl. Phys. Lett., 75, 1328 (1999).

[2] S.Oestreich, B. Kaulich, J. Susini, Rev. Sci. Instrum., 70, 1921 (1999).

[3] B. Niemann, in X-ray microscopy and Spectromicroscopy, J. Thieme et al. (eds.), Springer Verlag, IV-45 (1998).

[4] S. Oestreich, G. Rostaing, B. Niemann, B. Kaulich, M. Salome, J. Susini, R. Barrett, in 6th International Conference on X-ray microscopy, W.Meyer-Ilse, T.Warwick, D.Attwood (eds.), AIP Proceedings (Berkeley, Aug. 1999), vol. 507.

[5] M. Panitz, G. Schneider, M. Peuker, D. Hambach, B. Kaulich, S. Oestreich, J. Susini, G. Schmahl, in 6th International Conference on X-ray microscopy, W. Meyer-Ilse, T. Warwick, D. Attwood (eds.), AIP Proceedings (Berkeley, Aug. 1999), vol. 507.

[6] E. Di Fabrizio, L. Grella, M. Baciocchi, M. Gentili, L. Peschiaroli, L. Mastrogiacomo, R. Maggiora, J. Vac. Sci. Technol., B 14, 3855 (1996).

ACKNOWLEDGEMENTS

The authors thank L. André, R. Baker, P. Bernard, G. Berruyer, A. Koch, F. Demarcq, D. Fernandez, P. Noé, S. Ohlsson, D. Rolhion, G. Rostain, M. Soulier, F. Thurel, and H. Witsch for their invaluable technical assistance and contributions. The performance of this microscope benefits from the high-quality phase zones plates produced by E. Di Fabrizio, M. Panitz and P. Charalambous. The conception of the microscope was aided greatly by many hours of fruitful discussion with many collaborators, especially B. Niemann, G. Schneider, T. Wilhein, and W. Meyer-Ilse.

IN-VACUUM UNDULATORS

P. ELLEAUME, J. CHAVANNE AND P. VANVAERENBERGH

ESRF, MACHINE DIVISION

Following the successful operation of a prototype in-vacuum undulator on ID11, the ESRF has started the production of 4 in-vacuum undulator segments, of 2 m in length and with periods between 17 and 23 mm.

INTRODUCTION

The magnetic gap of undulators and wigglers, as for any other accelerator magnet (dipole, quadrupole,…), is a design parameter of major importance. The smaller the gap, the lower the current or the smaller the volume of magnetic material (permanent magnet or steel) needed to reach a given magnetic field. In the case of undulators, a reduction of the gap also allows a reduction of the spatial period which results in a shift of the radiation spectrum to higher energies. This is of prime interest in a number of scientific applications. In the classical and simplest approach, one uses a fixed-gap vacuum chamber and places the magnet blocks in the air outside the vacuum. At the ESRF, the smallest aperture left to the electron beam (beam stay-clear) is around 5-6 mm if one does not want to reduce the lifetime of the stored beam (see below). When taking into account the thickness of the chamber wall, the flatness and position errors, the result is a minimum gap in the range of 10-11 mm. So far the majority of ESRF beamlines are equipped with a 15 mm-thick chamber which permits a minimum gap around 16 mm. The first 10 mm chambers have met the mechanical specifications but the lack of distributed pumping has not allowed user operation for lengths exceeding 2 m. This is due to the Bremsstrahlung generated by the collision of the electrons with the residual gas. One way to avoid these difficulties is to place the permanent magnet blocks in the vacuum of the ring (in-vacuum undulator). This allows a minimum gap almost identical to the beam stay-clear. The idea of in-vacuum undulators can be traced to the early 1980's with an installation on the NSLS [1] ring and later BESSY [2]. The technology was re-examined with the installation of a 3.6 m-long device at the photon factory [3]. Then a real advance took place with the large-scale engineering development made at SPRING-8 [4]. SPRING-8 is presently operating more than 15 in-vacuum undulators each with a typical length of 4.5 m and a 30 m-long in-vacuum undulator is also under construction. Recently a short in-vacuum undulator (0.32 m) was installed at the NSLS [3]. The record minimum gap is 3.3 mm with a 10% lifetime penalty. Such a small gap is only possible due to the short length of

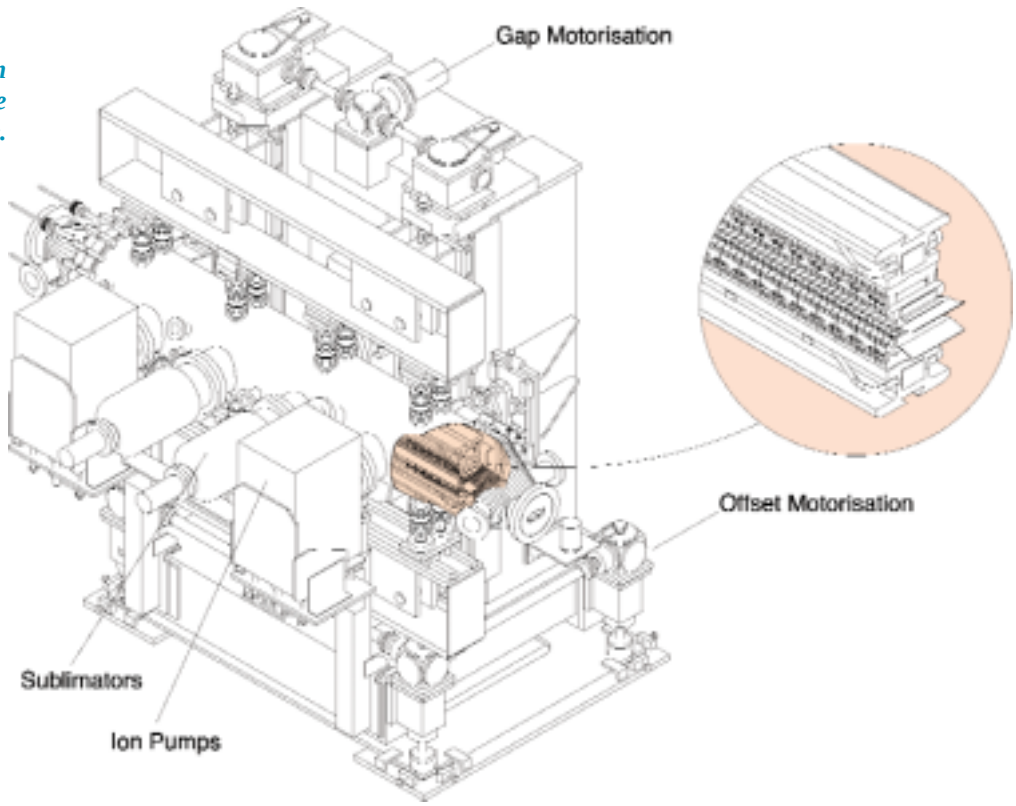

Fig. 1: Prototype in-vacuum undulator installed on the ID11 beamline.

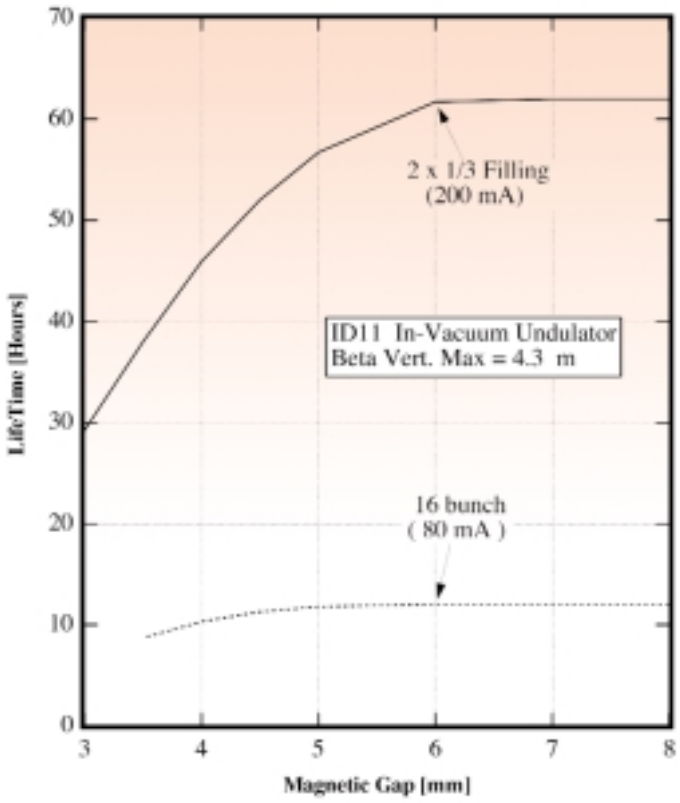

Fig. 2: Measured lifetime as a function of the magnetic gap of the prototype in-vacuum undulator.

undulator which allows the use of a small vertical beta function. Assuming an optimised beta function, the smallest gap achievable scales with the square root of the length of the undulator. For reasons of cost and resources, the development at the ESRF of this technology only started four years ago with the testing of a prototype Spring-8 undulator [6] followed by the construction of a prototype device [7]. We are now embarking on a large-scale programme of construction of such in-vacuum undulators. One should also mention that several new facilities of medium energy (Swiss Light Source, Canadian Light Source, Advanced Light Source ..) have chosen to build such in-vacuum undulators. Although they used to be considered a specialised and risky technology, in-vacuum undulators are now becoming much more common.

EXPERIENCE WITH THE ESRF PROTOTYPE

The prototype in-vacuum undulator in operation on ID11 is 1.6 m long with a period of 23 mm, and with a peak field higher than 1.1 T at the minimum operation gap of 5 mm. Figure 1 presents a 3-D view of the undulator, the support, the tank and pumping system. This undulator was designed to operate with the smallest gap that would be compatible with an acceptable reduction of the lifetime. Consequently, a significant number of the electrons lost in the ring are likely to hit the permanent magnet material. In view of the partial demagnetisation that was observed in 1993 on two conventional undulator segments (following a mis-steering of the booster beam), it was decided to use Sm_2Co_{17} material for the magnet blocks. The reduction of the field as a consequence of the use of Sm_2Co_{17} instead of NdFeB is equivalent to a 1 mm gap difference. A large pumping capacity was made available to the tank (860 l/s ion pump & 2000 l/s of titanium sublimation). As a result no measurable Bremsstrahlung could be observed on the beamline for any gap larger than 4.5 mm. Figure 2 presents the measured reduction of lifetime as a function of the magnetic gap in the 2 x 1/3 filling mode (200 mA) and 16 bunch mode (80 mA). No measurable lifetime reduction can be observed above 6 mm, however, a 5% lifetime reduction is recorded at 5 mm. Before the installation of this undulator, ID11 was operating a 1.2 T wiggler with a 125 mm period of the same length. The field was not shimmed due to a lack of time. Despite this, the new undulator produced more flux per unit surface at the primary slit for all energies below 70 keV, which has made the wiggler almost completely obsolete.

ENGINEERING DIFFICULTIES

Several engineering difficulties (vacuum, mechanical and magnetic) were encountered in the production of in-vacuum undulators. As all magnets must be coated to limit the degassing in UHV, nickel plating was used which resulted in a $9x10^{-11}$ static vacuum after bake-out at 120°C. Additionally, the magnets must be covered with a continuous conducting sheet (copper) to let the return current flow freely without heating the magnets. Continuity at the exits of the undulator must also be ensured. These exit transitions (called RF-Fingers) need to be flexible to allow a gap change in the range of 5-30 mm. Their perturbation on the beam is quantified in terms of an impedance which produces local heating (real part of the impedance) and is responsible for beam instabilities (imaginary part of the impedance). The highest temperature recorded on the prototype was 120°C at the junction between the RF-finger and the magnets. The connections between the upper and lower rigid girders (open air) and the magnet assemblies (in-vacuum) are made by 8 columns surrounded by bellows that must operate for a large number of cycles without leaking. Finally, the procedure for magnetic measurement and shimming had to be significantly modified because of the lack of lateral access for a Hall probe when the magnets are "in-vacuum".

FUTURE

The ESRF is presently embarking on the manufacture of four new in-vacuum undulator segments, each 2 metres-long with periods of between 17 and 23 mm. In view of the extra space required for the RF-fingers, the segment length has been increased from 1.6 m to 2 m in order to accommodate a maximum number of two segments. In the longer term, the manufacture of more in-vacuum undulators will be linked to the availability of 10 mm fixed gap chambers with a proper dynamic

vacuum. There are two main reasons for the use of in-vacuum undulators at the ESRF: Firstly, for a given K value (imposed by the tunability), an in-vacuum undulator can be built with a smaller period and a correspondingly higher photon energy of the fundamental and harmonics. This is of importance for beamlines where high brilliance at high photon energy is required. This is illustrated in Figure 3 which compares the ultimate brilliance of two fully tunable undulators with K=2.2, a 4 m long U28 in-vacuum operated with a minimum gap of 6 mm and a 5 m long U42 undulator with a minimum gap of 16 mm. The gain in brilliance is not significant at low energies, however, it grows very rapidly above 20 keV. Secondly, full tunability is not essential for a few ESRF beamlines, and in preference they are optimised for maximum flux on the fundamental around 12-14 keV. In-vacuum undulators are also well suited for such applications, this is illustrated by Figure 4.

As discussed earlier, in-vacuum undulators can compete with wigglers (ID11) due to their high field. Indeed, not all wiggler beamlines can benefit from such undulators since they have a very small divergence and are nevertheless limited in field and therefore in critical energy. Very high field wavelength shifters are far from being obsolete. The question has been raised of whether it is possible to build hard X-ray rings at 4-5 GeV more cheaply than the present 6-8 GeV rings by making extensive use of in-vacuum undulators instead of open-air undulators. This is partly true, but one should not forget that reducing the electron energy of a low emittance ring has a serious impact on the lifetime and the stability of the beam. ■

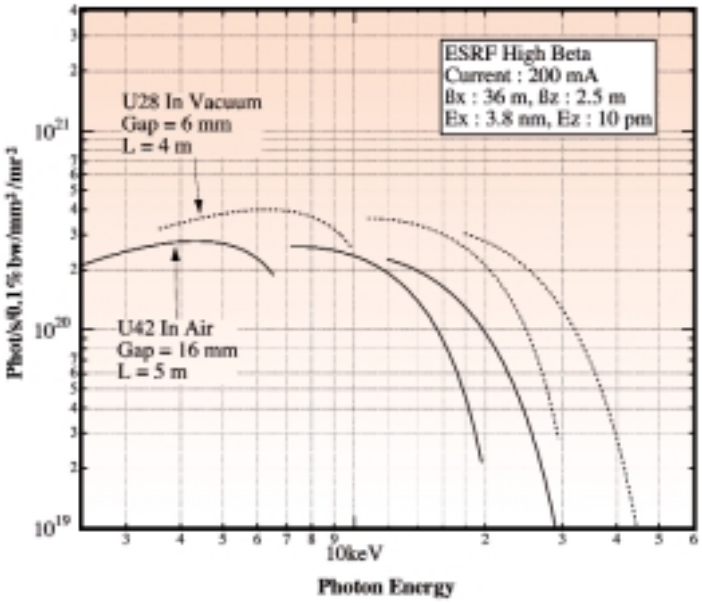

Fig. 3: Brilliance comparison between two fully tuneable undulators (K = 2.2) at a gap of 16 mm and 6 mm.

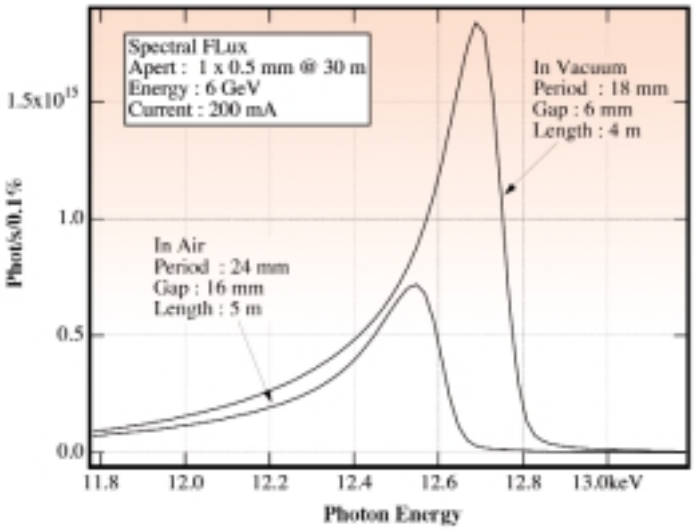

Fig. 4: Comparison of spectral flux in the fundamental for a 16 mm gap and 6 mm gap undultor. These undulators have a limited range of tunability and the period is optimised for a maximum flux around 1 Angstrom.

References

[1] H. Hsieh, S. Krinsky, A. Luccio, C. Pellegrini, A. Van Steenbergen, Nucl. Instr. and Methods, A208, 79-90 (1983).

[2] W. Gudat, J. Pfluegher, J. Chatzipetros, W. Peatman, Nucl. Instr. and Methods, A246, 50-53 (1986).

[3] S. Yamamoto, T. Shioya, M. Hara, H. Kitamura, X. Zhang, T. Mochizuki, H. Sugiyama, M. Ando, Rev. Sci. Instrum., 63, 400 (1992).

[4] T. Hara, T. Tanaka, T. Tanabe, X.M. Marechal, S. Okada, H. Kitamura, J. Synch. Rad., 5, 403-405 (1998).

[5] P.M. Stefan et al., J. Synch. Rad., 5, 417-419 (1998), see also P.M. Stefan et al., Nucl. Instr. and Methods, A412, 161 (1998).

[6] T. Hara et al., J. Sync. Rad., 5, 406-408 (1998).

[7] J. Chavanne, P. Elleaume, P. Van Vaerenbergh, Proc. of the 1999 Particle Accelerator Conference, p. 2662.

ACKNOWLEDGEMENTS

The authors would like to thank B. Plan from the Drafting Office who supervised the mechanical design work and R. Kersevan, M. Hahn, D. Schmied of the Vacuum Group for the design and handling of the vacuum equipment and also the Alignment Group.

The ESRF Newsletter is published by the European Synchrotron Radiation Facility
BP 220, F38043 Grenoble cedex
Editor: Dominique CORNUÉJOLS Tél (33) 4 76 88 20 25

Dépôt légal : 4eme trimestre 2000. Printed in France by Imprimerie du Pont de Claix. Layout by Pixel Project.